*FINAL*

# ISORROPIA: A NEW THERMODYNAMIC EQUILIBRIUM MODEL FOR MULTIPHASE MULTICOMPONENT INORGANIC AEROSOLS

**Athanasios Nenes**

Division of Marine and Atmospheric Chemistry, Rosenstiel School of Marine and Atmospheric Science, University of Miami, 4600 Rickenbacker Causeway, Miami, Florida, 33149, USA

**Christodoulos Pilinis***

Department of Environmental Science, University of the Aegean, Karadoni 17, Mytilene, GR-81100, Greece

**Spyros N. Pandis**

Departments of Chemical Engineering and Engineering and Public Policy, Carnegie Mellon University, Pittsburgh, Pennsylvania, 15213, USA

* To whom correspondence should be addressed.

## Abstract

A computationally efficient and rigorous thermodynamic model that predicts the physical state and composition of inorganic atmospheric aerosol is presented. One of the main features of the model is the implementation of mutual deliquescence of multicomponent salt particles, which lowers the deliquescence point of the aerosol phase.

The model is used to examine the behavior of four types of tropospheric aerosol (marine, urban, remote continental and non-urban continental), and the results are compared with the predictions of two other models currently in use. The results of all three models were generally in good agreement. Differences were found primarily in the mutual deliquescence humidity regions, where the new model predicted the existence of water, and the other two did not. Differences in the behavior (speciation and water absorbing properties) between the aerosol types are pointed out. The new model also needed considerably less CPU time, and always shows stability and robust convergence.



## Keywords

Inorganic aerosols, thermodynamic equilibrium, mutual deliquescence, ammonium salts, sodium salts, aerosol model

## Introduction

Atmospheric aerosols are airborne particles that are composed of water, inorganic salts, insoluble materials (dust, crustal material) organics (soot, VOC) and trace metals. The size of these particles cover a broad range, and the composition and mechanisms that generate them differ for each size section.

Knowledge of the physical state and composition of these particles is of great importance because of the role they play in important atmospheric processes. The major effect of aerosol is in the earth's climate (climate forcing), which is achieved by altering the radiation balance both through direct and indirect mechanisms. Direct forcing is the effect induced by scattering and absorption of solar radiation from the particles themselves. Indirect forcing is the effect of aerosols on cloud optical depth and albedo, caused by alteration of the available cloud condensation nuclei (CCN). Changes of CCN concentration affect the droplet size distribution, size and coverage of clouds on both a temporal and spatial scale. Specifically, an increase of CCN leads to smaller droplet sizes, yielding brighter and more reflective clouds. Estimating indirect forcing is of great importance, because of its significance in the planetary radiation budget. For example, marine boundary layer clouds contribute to about one third of the Earth's albedo (Charlson *et al.*, 1987). Because of the nonuniform geographical distribution of aerosols and the complex mechanisms which they are involved in, it is well recognized that aerosol production is the most uncertain and elusive of all anthropogenic activities affecting climate.

Marine aerosols also play an important role in the DMS sulfur cycle, by providing a medium for heterogeneous conversion of $SO_2$ to non-sea salt sulfate (nss). This pathway affects the available CCN (Russell *et al.*, 1994), and is one of the mechanisms involved in indirect climate forcing of

aerosols. Because of their interaction with electromagnetic radiation, aerosols also impair visibility. Due to their chemical composition, especially when mixed with polluted air rich in $SO_2$ and $NO_x$ from continental sources, these aerosols can produce acid rain, which causes structural erosion and degradation of soil and water quality. There has also been concern about the effect of acidic aerosol on public health (Saxena *et al.*, 1993).

Inorganic salts comprise 25-50% of dry total fine aerosol mass (Heintzenberg, 1989) and together with water consist a significant portion of the total aerosol mass (especially in high relative humidity environments). The inorganic salts found are mainly those of ammonium, sodium, sulfate, nitrate and chloride. Total particle concentrations are fairly uniform throughout the tropical regions, and range between 100 to 300 $cm^{-3}$ (Fitzgerald, 1991). The aerosol size distribution is characterized by 3 modes, the nuclei region ($D_p < 0.1\mu m$), accumulation mode ($0.1\mu m < D_p < 0.5\mu m$), and the coarse mode ($D_p > 0.5\mu m$) (e.g., Pandis *et al.*, 1995). Nuclei are generated by the homogeneous heteromolecular nucleation of $H_2SO_4$ vapor produced from the gas phase oxidation of $SO_2$ and methanosulfonic acids by OH radicals. Although the mechanism for developing the accumulation mode is still unclear, the prevailing hypothesis is that this section is the result of cloud formation and evaporation cycles (Pandis *et al.*, 1995). Cloud formation allows the heterogeneous oxidation of $SO_2$ to form sulfate in the droplets, reacting with sea salt that might exist in the cloud droplets. As a result, this increases the dry aerosol mass and changes the composition of cloud droplets. Coarse particles are mainly composed of sea salt, and are generated from the evaporation of sea water droplets produced from bubble bursting and wind-induced wave breaking. Coarse mode particles also contain small amounts of nitrate and mineral dust (normally up to 5% of sea salt mass) although occasionally, dust concentrations can reach very high levels, comparable to that of sea salt (Fitzgerald, 1991).

In order to calculate the mass and composition of aerosols, a common assumption made is that volatile species in the gas and aerosol phases are in chemical equilibrium. Although in many cases this has proven to be a valid assumption, there are situations in which the time needed to achieve chemical equilibrium is long compared to the time which local air and particles remain in contact. When this happens, the equilibrium approach is not valid and a model incorporating transfer processes should be applied (Wexler and Seinfeld, 1990; 1991). However, the cases in which such an approach is needed are limited to coarse particle sizes and cool environments (Wexler and Seinfeld, 1990; Meng and Seinfeld, 1996). Experimental evidence for the non-equilibrium state has been found (Allen *et al.*, 1989), but for marine aerosols and/or warmer environments, the thermodynamic equilibrium assumption is valid and has been experimentally confirmed (Hildemann *et al.*, 1984; Quinn *et al.*, 1992).

There has been substantial work in the past in terms of thermodynamic aerosol models. Bassett and Seinfeld (1983), developed EQUIL in order to calculate the aerosol composition of the ammonium-sulfate-nitrate-water aerosol system. They later introduced an improved version, KEQUIL, to account for the dependence of the partial vapor pressure on the sphericity of the particles, the so-called Kelvin effect (Bassett and Seinfeld, 1984).

Another widely used model for the sulfate-nitrate-ammonia-water system is MARS (Saxena *et al.*, 1986) that aimed at reducing the computational time while maintaining reasonable agreement with EQUIL and KEQUIL. MARS was developed for incorporation into larger aerosol models, so speed was a major issue. The main feature of MARS was the division of the whole aerosol species regime into subdomains, in order to minimize the viable species in each one. Since each domain contains fewer species than the entire concentration domain does, the number of equations solved is reduced,

thus, speeding up the solution process. A major drawback of MARS is that it uses thermodynamic properties (equilibrium constants, activity coefficients) at 298.15K, thus affecting the distribution of volatile species (nitrates) between the gas and the particulate phases, if calculations are done at a different temperature. All the simplifications rendered MARS about four hundred times faster than KEQUIL and sixty times faster than EQUIL.

The major disadvantage of the previous three models was the neglect of sodium and chloride species, which are major components of marine aerosols. These species were first incorporated into the SEQUILIB model (Pilinis and Seinfeld, 1987). SEQUILIB used a computational scheme similar to that of MARS. It also presented an algorithm for calculating the distribution of volatile species among particles of different sizes so that thermodynamic equilibrium is achieved between all the particles and the gas phase.

Recently, Kim *et al.* (1993) developed SCAPE, which implements a domain-oriented solution algorithm similar to that of SEQUILIB, but with updated thermodynamic data for the components. SCAPE also calculates the pH of the aerosol phase from the dissociation of all weak and strong acid/base components, and includes the temperature dependence of single salt deliquescence points using the expressions derived by Wexler and Seinfeld (1991). SCAPE embodied the main correlations available for calculating multicomponent solution activity coefficients, and let the user select which one should be used. SCAPE always attempts to solve for a liquid phase, by using SEQUILIB to calculate approximate concentrations that serve as a starting point for the iterative solution of the full equilibrium problem. Because of this approach, SCAPE can predict the presence of water even at very low ambient relative humidities. In certain cases, the activity coefficients may lower the solubility product enough so that there is no solid precipitate predicted. There is no relative humidity

"boundary" that could inhibit this, so a liquid phase may be predicted for relative humidities as low as 20%. There are two ways to solve this problem. Either certain assumptions must be made about the physical state of the aerosol at low realtive humidities (like MARS and SEQUILIB), or the full minimization problem must be solved.

A different approach has been followed by Jacobson *et al.* (1996) in their model, EQUISOLV. The equilibrium concentrations are calculated by numerically solving each equilibrium equation separately, based on an initial guess for the concentrations. After solving each equation, the solution vector is updated and the new values are used to solve the remaining equations. This sequence is repeated over and over, until concentrations of all species converge. This open architecture makes it easy to incorporate new reactions and species, however, the general nature of the algorithm could potentially slow down the solution process, when compared to the domain approach used in MARS, SEQUILIB and SCAPE. Solubility products are used to determine the presence of solids. For this reason, EQUISOLV, just like SCAPE, can predict the presence of water even at very low relative humidities. Even for cases in which a solid aerosol is predicted, a negligible amount of water is assumed to exist, in order to estimate the vapor pressure of species in the aerosol phase. While this should not affect the results (because there is too little water to affect the solution), additional computations are required, which could increase CPU time. EQUISOLV has been used to study the formation and composition of stratospheric clouds (Jacobson *et al.*, 1996).

A major weakness in all the models presented lies in the way they treat the transition between the aqueous and solid aerosol phases. A solid particle transforms into an aqueous solution when the relative humidity reaches a specific level, characteristic of each salt. This relative humidity is called Deliquescence Relative Humidity (DRH). It has been shown both theoretically (Wexler *et al.*, 1990;

Potukuchi and Wexler, 1995a, 1995b), and experimentally (Tang and Munkelwitz, 1993) that the deliquescence relative humidity (DRH) of a salt mixture is lower than the minimum DRH of each component:

$$DRH\left(salt_1, salt_2, \ldots salt_n\right) < \min\left\{DRH_{salt_1}, DRH_{salt_2}, \ldots DRH_{salt_n}\right\} \quad (1)$$

The DRH of the mixture does not have a unique value, but is a function of mixture composition. The minimum DRH is known as Mutual Deliquescence Relative Humidity (MDRH). At the MDRH the aqueous phase is saturated with respect to all the salts, and so it is the only RH in which an aqueous solution can coexist with a precipitate composed of all the aerosol salts. The system is said to be in a Mutual Deliquescence Region (MDR), when the relative humidity is:

$$MDRH\left(salt_1, salt_2, \ldots salt_n\right) \leq RH < \min\left\{DRH_{salt_1}, DRH_{salt_2}, \ldots DRH_{salt_n}\right\} \quad (2)$$

Neglecting mutual deliquescence leads to the erroneous prediction of a dry aerosol for cases when the RH lies in a MDR. This potentially can affect the predicted role of aerosols, since the presence of aerosol water affects the partitioning of volatile species and particle size. For example, Pilinis *et al.* (1995) performed a sensitivity analysis to determine the most important parameter affecting the direct forcing of aerosols. The conclusion was that relative humidity, i.e. water uptake, was the parameter that mostly affected aerosol optical properties. So, at least for aerosols in a MDR, the predicted forcing can change notably when mutual deliquescence is considered. This is further supported by the fact that accumulation mode particles, which are optically the most active, are multicomponent mixtures.

Another issue lies in the constant need for faster and more efficient solution algorithms, that try to avoid simplifying assumptions without sacrificing speed. Numerical stability and robustness are desired characteristics of an algorithm, and models satisfying these constraints make them suitable for large (3D) circulation and urban airshed models.

This paper presents an improved thermodynamic equilibrium aerosol model, referred to as ISORROPIA, "equilibrium" in Greek, which attacks all the problems addressed above. Besides incorporating an algorithm for mutual deliquescence regions, the solution process was optimized for speed and robustness. The system modeled by ISORROPIA includes ammonium, sodium, chloride, nitrate, sulfate and water, which are partitioned between gas, liquid and solid phases. The aerosol particles are assumed to be internally mixed, meaning that all particles of the same size have the same composition. Since the significant portion of aerosol mass is in diameter sizes much larger than 0.1 μm, the Kelvin effect is neglected (Bassett and Seinfeld, 1984).

In the following section, the equilibrium theory used is presented together with all the model-specific reactions and assumptions. ISORROPIA is then used to study the behavior of four distinct types of aerosols, and the predictions are compared to those of two other models, SCAPE and SEQUILIB.

## Aerosol Equilibrium Thermodynamics

The state of chemical equilibrium in a closed system, which in our case is the aerosol-gas phase system, for a constant temperature $T$, and pressure $p$, is that the total free energy of the system, $G$, is at a minimum. This is satisfied if and only if (Denbigh, 1981):

$$\sum_i \nu_{ij}\mu_i = 0, \text{ for all reactions } j \quad (3)$$

where $\nu_{ij}$ is the stoichiometric coefficient of the *i*-th species in the *j*-th reaction and $\mu_i = \left(\frac{\partial G}{\partial n_i}\right)_{T,p,n_c}$ is the chemical potential of species *i*. The following section discusses the expressions used for calculating $\mu_i$ and derives the expressions used in ISORROPIA.

## Chemical Potentials and Equilibrium Constants

The chemical potential of a species *i* is given by the expression:

$$\mu_i = \mu_i^o(T) + RT \ln a_i \quad (4)$$

where $\mu_i^o(T)$ is the standard chemical potential for 1 atm and temperature *T* (in K), *R* is the universal gas constant and $a_i$ the activity of the *i*-th species. For solids, $a_i = 1$. For ideal gases $a_i = p_i$, where $p_i$ is the partial pressure of the *i*-th species. For aqueous solutions of electrolytes, $a_i = \gamma_i^{(\nu_+ + \nu_-)} m_+^{\nu_+} m_-^{\nu_-}$, where $\gamma_i$ is the activity coefficient of species *i* in water, $\nu_+$ and $\nu_-$ are the moles of cations and anions, respectively, released per mole of electrolyte and $m_+$, $m_-$ are their molalities, respectively. For electrolytes, the standard chemical potential is related to the standard chemical potentials of the cations and anions, $\mu_{i_+}^o(T), \mu_{i_-}^o(T)$ with the relationship:

$$\mu_i^o(T) = \nu_+ \mu_{i_+}^o(T) + \nu_- \mu_{i_-}^o(T) \quad (5)$$

After substituting (4) into (3) and rearranging:

$$\prod_i a_i^{\nu_{ij}} = K_j(T) \tag{6}$$

where $K_j(T)$ is the equilibrium constant of the *j*-th reaction,

$$K_j(T) = \exp\left[-\frac{\sum_i \nu_{ij}\mu_i^o(T)}{RT}\right] \tag{7}$$

The system of Equations (6) is the one that determines the equilibrium concentration of all species *i*.

To determine the equilibrium constant at a temperature *T*, the Van't Hoff equation is used:

$$\frac{d\ln K(T)}{dT} = \frac{\Delta H^o(T)}{RT^2} \tag{8}$$

where $\Delta H^o(T)$ is the standard enthalpy change of the reaction at temperature *T* (Denbigh, 1981). For a small temperature range, the change in this quantity can be approximated by:

$$\Delta H^o(T) = \Delta H^o(T_o) + \Delta c_p^o(T - T_o) \tag{9}$$

where $\Delta H^o(T)$ is the standard enthalpy change at a reference temperature (usually 298.15K) and $\Delta c_P^o(T)$ is the change of heat capacity at $T_o$. By substituting (9) into (8) and integrating from $T_o$ to *T*, the expression for $K(T)$ is obtained:

$$K(T) = K_o \exp\left[-\frac{\Delta H^o(T_o)}{RT_o}\left(\frac{T_o}{T} - 1\right) - \frac{\Delta c_p^o}{R}\left(1 + \ln\left(\frac{T_o}{T}\right) - \frac{T_o}{T}\right)\right] \tag{10}$$

where $K_o$ is the equilibrium constant at the reference temperature $T_o$.

## Water Activity

The ambient relative humidity can be assumed to be uninfluenced by the deliquescence of aerosol particles because of the large amount of water vapor in the atmosphere (Bassett and Seinfeld, 1983). Under this assumption, and by neglecting the Kelvin effect, phase equilibrium between gas and aerosols gives that the water activity, $a_w$ , is equal to the ambient relative humidity (Bassett and Seinfeld, 1983):

$$a_w = RH \tag{11}$$

where *RH* is expressed on a fractional (0-1) scale.

The ZSR correlation (Robinson and Stokes, 1965) is used to calculate the water content of the aerosols:

$$\sum_i \frac{m_i}{m_{oi}(a_w)} = 1 \tag{12}$$

where $m_i$ is the molality of the *i*-th electrolyte in the multicomponent solution and $m_{oi}(a_w)$ is the molality of an aqueous solution of species *i* with the same water activity as the multicomponent solution. Equation (12) is rewritten in a way to explicitly calculate aerosol water content. By definition, molality is $m_i = \frac{M_i}{W}$, where $M_i$ is the molar concentration of species *i* in the air (mol $m^{-3}$ air) and *W* is the mass concentration of aerosol water in the air (kg $m^{-3}$ air). So by substituting $m_i$ into Equation (12), the water content of the aerosols, *W* is calculated by:

$$W = \sum_i \frac{M_i}{m_{oi}(a_w)} \tag{13}$$

## Activity Coefficients

Most of the methods that predict the activity coefficients of a multicomponent solution are empirical, or semi-empirical and typically use the activity coefficients of single-electrolyte solutions of the same ionic strength. Kim *et al.*, (1993) compared predictions of binary and multicomponent mixture activity coefficients using models by Bromley (1973), Pitzer and Mayorga (1973) and Kusik and Meissner (1978) with available experimental data. The conclusion was that binary coefficients should be calculated using the Kusik and Meissner method, while there is no conclusive evidence for the superiority of any method for multicomponent solutions. The reason for this lies in the fact that activity measurements for multicomponent systems are available for relatively low ionic activities (up to 6M), while much higher ionic activities are found in aerosols (up to 30 M), especially when the ambient relative humidity is low.

The multicomponent activity coefficients in ISORROPIA are calculated using Bromley's formula:

$$\log \gamma_{12} = -A_\gamma \frac{z_1 z_2 I^{1/2}}{1 + I^{1/2}} + \frac{z_1 z_2}{z_1 + z_2}\left[\frac{F_1}{z_1} + \frac{F_2}{z_2}\right] \qquad (14)$$

where $\gamma_{12}$ is the activity coefficient of Cation 1 and Anion 2, $A_\gamma$ is the Debye-Huckel constant, which has a value of 0.511 $kg^{0.5}$ $mol^{-0.5}$ at 298.15 K, and,

$$F_1 = Y_{21}\log\gamma_{12}^o + Y_{41}\log\gamma_{14}^o + Y_{61}\log\gamma_{16}^o + \ldots + \frac{A_\gamma I^{1/2}}{1 + I^{1/2}}\left[z_1 z_2 Y_{21} + z_1 z_4 Y_{41} + z_1 z_6 Y_{61} + \ldots\right] \qquad (15)$$

$$F_2 = X_{12}\log\gamma_{12}^o + X_{32}\log\gamma_{32}^o + X_{52}\log\gamma_{52}^o + \ldots + \frac{A_\gamma I^{1/2}}{1 + I^{1/2}}\left[z_1 z_2 X_{12} + z_3 z_2 X_{32} + z_5 z_2 X_{52} + \ldots\right] \qquad (16)$$

$$Y_{21} = \left( \frac{z_1 + z_2}{2} \right)^2 \frac{m_2}{I} \tag{17}$$

$$X_{12} = \left( \frac{z_1 + z_2}{2} \right)^2 \frac{m_1}{I} \tag{18}$$

$I$ is the ionic strength of the solution,

$$I = \frac{1}{2} \sum_i m_i z_i^2 \tag{19}$$

$z_i$ is the absolute charge of ionic species $i$, and $\gamma_{ij}^o$ is the mean ionic activity coefficient of the binary pair *i-j* (binary activity coefficient) for a solution that contains only *i-j* ions at the ionic strength of the multicomponent solution. In Equations (14) to (18), odd subscripts refer to cations, while even subscripts refer to anions.

The binary activity coefficients needed in Equations (15) and (16) are calculated from the relationship (Kusik and Meissner, 1978):

$$\log \gamma_{12}^o = z_1 z_2 \log \Gamma^o \tag{20}$$

where

$$\Gamma^o = \left[ 1 + B(1 + 0.1I)^q - B \right] \Gamma^* \tag{21}$$

$$B = 0.75 - 0.065q \tag{22}$$

$$\log \Gamma^* = \frac{-0.5107 I^{1/2}}{1 + CI^{1/2}} \tag{23}$$

$$C = 1 + 0.055q\exp\left(-0.023I^3\right) \tag{24}$$

$q$ is a parameter specific for each salt.

## Deliquescence of Single Salt Particles

A solid particle transforms into an aqueous solution when the relative humidity reaches a specific level, characteristic for each salt. This is known as the relative humidity of deliquescence (DRH). The DRH is a function of temperature, and for a small $T$ range can be calculated by (Wexler and Seinfeld, 1991):

$$ln\frac{DRH(T)}{DRH(T_o)} = -\frac{M_w m_s L_s}{1000R}\left(\frac{1}{T} - \frac{1}{T_o}\right) \tag{25}$$

where $T_o$ is the temperature in which the DRH is known (usually 298.15 K), $M_w$ is the molecular weight of water, $m_s$ is the molality of the saturated solution at temperature $T_o$, $R$ is the universal gas constant, $L_s = \Delta H_{cr} - \Delta H_{aq}$ is the latent heat of fusion for the salt from a saturated solution, $\Delta H_{cr}$ is the standard heat of formation of the crystalline phase and $\Delta H_{aq}$ is the standard heat of formation of the species in aqueous solution. Tang and Munkelwitz (1993), proposed a more elaborate expression, but for moderate temperature ranges, they showed that Equation (25) is adequate.

## Deliquescence of Multicomponent Salt Particles

As pointed out before, the minimum relative humidity in which a multicomponent mixture can deliquesce is known as mutual deliquescence relative humidity (MDRH). This point is also known as the “eutonic point” (Tang and Munkelwitz, 1993) and corresponds to the mixture with a

composition that minimizes water activity. Below this point, a solid phase is thermodynamically favored. So consequentially, MDRH points can be used to determine when an aqueous phase is possible.

To estimate the aerosol composition in a mutual deliquescence region, the full minimization problem must be solved (Potukuchi and Wexler, 1995a, 1995b). Since ISORROPIA is intended to be as fast as possible for incorporation in 3D models, an alternative approach was used for the mutual deliquescence region. The aerosol composition is assumed a weighted mean of two states, one in which there is no water ("dry" state) and one in which the most hygroscopic salt (i.e. that with the lowest DRH) is completely dissolved ("wet" state). The weighting factor, *c*, is defined as:

$$c = \frac{RH - RH_{wet}}{MDRH - RH_{wet}} \tag{26}$$

where *MDRH* is the mutual deliquescence relative humidity for the given mixture, and $RH_{wet}$ is the DRH of the most hygroscopic salt in the mixture.

The weighting algorithm used is:

- Aerosol water content is proportional to the weighting factor, and specifically is equal to $(1-c)(H_2O)_{wet}$, where $(H_2O)_{wet}$ is the water content of the "wet" solution, expressed in kg $m^{-3}$ air.

- The concentration of any solid salt or gaseous species $\Phi$, is a weighted mean of both solutions, i.e.: $(\Phi) = c(\Phi)_{dry} + (1-c)(\Phi)_{wet}$ where concentrations are expressed in moles $m^{-3}$ air. The subscripts "*dry*" and "*wet*" refer to the dry and wet solutions respectively.

- Concentrations of ionic species are calculated from the dissolved solids and gases. This ensures mass conservation and electroneutrality. For any given species $\Phi$, (solid salt or gas), the amount dissolved in the aqueous phase is equal to $(1-c)\left[(\Phi)_{dry} - (\Phi)_{wet}\right]$. As one can observe, the dissolved species are proportional to the amount of aerosol water

The MDRH points for calculating the weights are obtained from phase maps calculated by Potukuchi and Wexler (1995a, 1995b). These maps cover the majority of all possible MDRH points. However, there are salt mixtures where MDRH information could not be found. Due to this lack of information, it is assumed that the salt mixture has the same MDRH of a another mixture with known deliquescence properties. The values of the salt mixture system that most closely approximated it (i.e. most similar in composition) was used. For example, the MDRH point for a $NH_4NO_3$-$NH_4Cl$-$Na_2SO_4$-NaCl-$NaNO_3$ mixture is not known. Since the MDRH of it has to be lower than the DRH of all the salts, a mixture containing the salts with the lowest DRH (i.e. the nitrates and/or chlorides) should at least approximately have the same MDRH as the mixture in question. A $NH_4NO_3$ -$NH_4Cl$-NaCl-$NaNO_3$ system, according to Potukuchi and Wexler (1995) has a MDRH of 50%. So this is assumed to be the MDRH of the mixture in question.

The temperature dependence of MDRH is given by an equation similar to (25):

$$\ln\frac{MDRH(T)}{MDRH(T_o)} = -\frac{M_w\sum m_{si}L_{si}}{1000R}\left(\frac{1}{T}-\frac{1}{T_o}\right) \qquad (27)$$

where $T_o$ is the temperature in which the MDRH is known (usually 298.15 K), $M_w$ is the molecular weight of water, $m_{si}$ is the molality of salt $i$ of the saturated solution at temperature $T_o$, $R$ is the universal gas constant, $L_{si} = \Delta H_{cri} - \Delta H_{aqi}$ is the latent heat of fusion for salt $i$ from a saturated

solution, $\Delta H_{cri}$ is the standard heat of formation of the crystalline phase and $\Delta H_{aqi}$ is the standard heat of formation of the species in aqueous solution. Equation (27), just like Equation (25), is a simplified version of an equation given by Tang and Munkelwitz (1993), but is sufficient for our calculations.

## The system modeled by ISORROPIA

ISORROPIA models the sodium - ammonium - chloride - sulfate - nitrate - water aerosol system. The possible species for each phase are:

Gas phase: $NH_3$, $HNO_3$, HCl, $H_2O$

Liquid phase: $NH_4^+$, $Na^+$, $H^+$, $Cl^-$, $NO_3^-$, $SO_4^{2-}$, $HSO4^-$, $OH^-$, $H_2O$

Solid phase: $(NH_4)_2SO_4$, $NH_4HSO_4$, $(NH_4)_3H(SO_4)_2$, $NH_4NO_3$, $NH_4Cl$, NaCl, $NaNO_3$, $NaHSO_4$, $Na_2SO_4$, $H_2SO_4$

Table I presents the fifteen equilibrium reactions used in ISORROPIA, together with the equilibrium and temperature dependence constants. The thermodynamic properties needed in the coefficients in Equation (10) are given by Kim *et al.*, (1993) and are shown in Table II.

Because sulfuric acid has a very low vapor pressure, it is reasonable to assume that it resides completely in the aerosol phase. The same assumption is made for sodium. Depending on the amount of sodium and ammonia, the sulfates can either be completely or partially neutralized. There is also the possibility of complete neutralization of sulfuric acid by sodium alone. In each of these cases, the possible species are different. In order to determine which case is considered, two parameters are defined:

$$R_{SO_4} = \frac{\left[Na^+\right] + \left[NH_4^+\right]}{\left[SO_4^{-2}\right]},\ R_{Na} = \frac{\left[Na^+\right]}{\left[SO_4^{-2}\right]} \tag{28}$$

$R_{SO_4}$ is known as the sulfate ratio, while $R_{Na}$ is known as the sodium ratio. The concentrations are expressed in molar units. Based on the value of these two ratios, four types of aerosols are defined:

- Sulfate rich (free acid): This is when $R_{SO_4} < 1$. The sulfates are in abundance and part of it is in the form of free sulfuric acid. In this case, there is always a liquid phase, because sulfuric acid is extremely hygroscopic (i.e., DRH is 0%).

- Sulfate rich (non free acid): This is when $1 \le R_{SO_4} < 2$. There is enough ammonia and sodium to partially (but not fully) neutralize the sulfates. The sulfates are a mixture of bisulfates and sulfates, the ratio of which is determined by thermodynamic equilibrium.

- Sulfate poor, Sodium poor: $R_{SO_4} \ge 2$; $R_{Na} < 2$. There is enough ammonia and sodium to fully neutralize the sulfates, but sodium is not enough to neutralize sulfates by itself. In this case, excess ammonia can react with the other species ($HNO_3$, HCl) to form volatile salts.

- Sulfate poor, Sodium rich: $R_{SO_4} \ge 2$; $R_{Na} \ge 2$. There is enough sodium to fully neutralize the sulfates. In this case, ammonia and excess sodium can react with the other gaseous species ($HNO_3$, HCl) to form salts, while no ammonium sulfate is formed (since all sulfates have been neutralized with sodium).

The possible species for each aerosol type are displayed in Table III. Values of the Kusik-Meissner activity parameter *q* were obtained from Kim *et al.* (1993) and are given in Table IV. For

species which the $q$ was not available, rules used by Kim *et al.* (1993) were applied. Water activity data used for the ZSR correlation were obtained from Pilinis and Seinfeld (1987). The DRH at reference temperature (298.15K) and the thermodynamic data needed for calculating $L_s$ were obtained from Kim *et al*., (1993), while the molalities of the saturated solution were obtained from Pilinis and Seinfeld (1987) and Wexler and Seinfeld (1990). The value of DRH and the temperature dependence coefficients for species in ISORROPIA are given in Table V.

MDRH points for 298.15K and the temperature dependence coefficients are given in Table VI. Thermodynamic data needed for calculating $L_s$ in Equation (27) was obtained from Kim *et al*., (1993), while the saturation molalities $m_{si}$ were calculated from the ZSR correlation, after obtaining the ion concentration ratios at the MDRH point from maps given by Potukuchi and Wexler (1995a, 1995b). MDRH points could not be found for $NH_4NO_3$, $(NH_4)_2SO_4$, $Na_2SO_4$, $NH_4Cl$ and $NH_4NO_3$, $NH_4Cl$, $Na_2SO_4$, NaCl, $NaNO_3$ mixtures. For these cases, the MDRH of the $NH_4NO_3$, $NH_4Cl$, $NaNO_3$ system (MDRH=50%) was used.

Inputs needed by ISORROPIA are the total concentrations of Na, $NH_3$, $HNO_3$, HCl and $H_2SO_4$ together with the ambient relative humidity and temperature. Then, based on the sulfate and sodium ratios, and the relative humidity, the appropriate subset of equilibrium equations (which correspond to the possible species for the conditions specified), together with mass conservation, electroneutrality and Equations (11) and (13) are solved to yield the equilibrium concentrations.

## Solution algorithm

Special provision was taken in order to make ISORROPIA as fast and computationally efficient as possible. The system of nonlinear equations for each subdomain were ordered and written in a way so that analytical solutions could be obtained for as many equations as possible. This way, the equations needing a numerical solution are minimized. The number of iterations performed during the numerical solution determines to a large degree how fast the model will be. So by minimizing the equations that need numerical solution, the model considerably speeds up. Using this approach, most cases in ISORROPIA are solved using only one level of iteration. The bisection method was used for obtaining the solution, since other faster solution algorithms, e.g. Newton, could not guarantee convergence. Even though SEQUILIB is more simplistic and thus, potentially faster, it will be proved to be slower. This is mainly because SEQUILIB solves more equations numerically and uses nested iteration procedures of two (and sometimes three) levels when solving the equations. Another factor that speeds up ISORROPIA is that binary activity coefficients are not calculated during runtime. The program uses an internal database with precalculated binary activity coefficients for each salt and for a wide range of ionic strengths. During model calculations, ISORROPIA does not spend time recalculating the coefficients, but simply queries the internal database, based on the ionic strength of the aqueous phase. This speeds up ISORROPIA by a factor of about two.

## Comparison study

A series of runs were performed in order to compare the predictions of ISORROPIA with two other models, SCAPE and SEQUILIB. In these runs, four types of aerosols were considered: urban, remote continental, non-urban continental and marine (Heintzenberg, 1989; Fitzgerald, 1991). This classification, just like any other, is qualitative, since there are no clear-cut patterns that differentiate

each type. Even for a particular aerosol class, there is significant variability found in composition, concentration and size distribution.

Remote continental aerosol originates from particles emitted by the biosphere (pollen, plant waxes) and the secondary oxidation products of biogenic gases (terpenes, etc.) (Deepak and Gali, 1991). Urban aerosol is strongly anthropogenic in origin, the main source being combustion products. This aerosol is composed mainly of sulfate, nitrates, ammonium and elemental and organic carbon (e.g., Pandis *et al.*, 1995). Non-urban continental aerosol is the result of mixing anthropogenic sulfate with background continental aerosol. The aerosol can be fairly acidic from the presence of nitric or sulfuric acids. Marine aerosol is composed largely of sea salt, while sulfate exists mainly from the gas-to-particle conversion of biogenic sulfur compounds (e.g., DMS). Other species found in marine aerosol are ammonium, nitrates and crustal materials (dust).

Total concentrations for the different aerosol types used in this study are given in Table VII. These concentrations were selected so that the amount of species in the aerosol phase are comparable to levels given by Fitzgerald *et al.*, (1991) for the marine aerosol and Heintzenberg (1989) for the other three types. The ambient temperature was fixed at 298.15K, while the relative humidity varied from 30% to 90% with an incremental step of 1%. The runs were performed on a DEC Alphastation 500/266MHz Workstation.

The urban aerosol case is a sulfate poor, sodium poor system. As a result, the aerosol phase is expected to consist primarily of ammonium sulfate and ammonium nitrate. As shown in Table VI, this dual salt mixture has a MDRH of 60%, while ammonium nitrate and ammonium sulfate deliquesce at relative humidities of 61.8% and 79.9%, respectively (Table V). So, according to Equation (2), there is a mutual deliquescence region for relative humidities between 60% and 61.8%. Figure 1 shows the plot of predicted aerosol water content against relative humidity, for the urban aerosol case. For

relative humidities below 60%, all models predict a solid aerosol (no water). When the RH reaches 60%, ISORROPIA predicts water, as a result of being in the mutual deliquescence region, while SEQUILIB and SCAPE do not. For humidities greater than 61.8%, SEQUILIB predicts water from the deliquescence of ammonium nitrate. SCAPE calculates significant aerosol water for relative humidities greater than 70%. This discrepancy is attributed to the different amount of aerosol nitrate which each model calculates, because the presence of nitrates drives water into the aerosol (at least for relative humidities below the DRH of ammonium sulfate). Figure 2 shows a plot of aerosol nitrate against relative humidity. These curves and the corresponding water curves of Figure 1 follow the same pattern. ISORROPIA predicts the existence of nitrates in the mutual deliquescence region (RH between 60% and 61.8%), while SEQUILIB predicts nitrates and water above the DRH of ammonium nitrate. On the other hand, SCAPE predicts nitrates and water only for relative humidities above 70%. Aerosol $SO_4^{2-}$ ion, which is generated from the dissolution of ammonium sulfate, is plotted as a function of relative humidity in Figure 3. SEQUILIB predicts complete dissolution of sulfates when ammonium nitrate deliquesces at 61.8% relative humidity. ISORROPIA predicts that ammonium sulfate begins dissolving at 60% relative humidity, in the mutual deliquescence region, and completely dissolves at 66%. SCAPE predicts total dissolution of ammonium sulfate for RH>70%. As relative humidity increases, SCAPE and ISORROPIA calculate a drop in the $SO_4^{2-}$ concentration. This is because as the water content increases and the salt solution is diluted, gas phase nitric acid is dissolved and $H^+$ ions are produced. Because of this, sulfate ions are consumed in order to generate bisulfates and maintain the thermodynamic equilibrium between them, according to Reaction 1 in Table I. For sulfate poor cases, SEQUILIB does not consider the equilibrium between bisulfates and sulfates, and so there is no drop seen in the sulfate level.

The remote continental aerosol case is a sulfate poor, sodium poor system. As a result, the aerosol is expected to consist primarily of ammonium sulfate and ammonium nitrate. This case displays a behavior similar to the urban aerosol case, which is not surprising since the sulfate and sodium ratios are almost identical (Table VII). Figure 4 shows the aerosol water content plotted against relative humidity, while Figure 5 presents the total aerosol nitrate against relative humidity. If one compares Figure 1 with Figure 4, it can be seen that the remote continental aerosol has more water than the urban case (at a given relative humidity). This is anticipated, because there is more sulfate mass in the remote continental aerosol. Also, as shown in Figure 5, SEQUILIB generally predicts more nitrate than the other two models. This is from the fact that SEQUILIB uses a higher value for the nitrate equilibrium constant in Reaction 4 (Table I), and so tends to partition more nitrate in the aerosol phase. In this case however, the increase in nitrate mass is relatively small and does not significantly affect the aerosol water content. This is verified by the water curves for ISORROPIA and SEQUILIB, which agree very well for RH > 61.8%.

The non-urban continental aerosol case is a sulfate poor, sodium poor system. As a result, the aerosol phase is expected to consist primarily of ammonium sulfate and ammonium nitrate. There is also a small amount of sodium and chloride, which will yield sodium sulfate, and possibly ammonium chloride. As shown in Table VI, a mixture of these four salts has a MDRH of 50%, while the minimum DRH of each component salt is that of ammonium nitrate, which is 61.8% (Table V). So, according to Equation (2), the mutual deliquescence region is for relative humidities between 50% and 61.8%. Figure 6 is a plot of predicted aerosol water content against relative humidity. For relative humidities below 50%, all models predict a solid aerosol (no water). When the RH reaches 50%, ISORROPIA predicts water, as a result of being in the mutual deliquescence region described above, while SEQUILIB and SCAPE do not. For humidities greater than 61.8%, SEQUILIB predicts water

due to the deliquescence of ammonium nitrate. SCAPE calculates significant aerosol water for relative humidities greater than 68%. This discrepancy is attributed to the different aerosol nitrate calculated by each model, because the presence of nitrates drives water into the aerosol (at least for relative humidities below the DRH of ammonium sulfate).

Figure 7 shows a plot of aerosol nitrate against relative humidity. These curves and the corresponding water curves of Figure 6 follow the same pattern: ISORROPIA and SEQUILIB predict nitrates, while SCAPE does not for relative humidities below 68%. However, when RH>68%, SCAPE calculates a significant amount of nitrates that agrees well with ISORROPIA. The higher nitrate levels calculated by SEQUILIB is due to the higher value of the nitrate equilibrium constant. The excess nitrate mass in SEQUILIB is significant enough to affect the water content, making the water levels slightly higher than in the two other models (Figure 6). Aerosol $SO_4^{2-}$ ions generated from the dissolution of sulfate salts is plotted as a function of relative humidity in Figure 8. SEQUILIB predicts complete dissolution of sulfates when ammonium nitrate deliquesces at RH=61.8%, while ISORROPIA starts to dissolve sulfates at RH=60%, in the mutual deliquescence region, and is completely dissolved at RH=68%. SCAPE predicts total dissolution of sulfates at RH>69%. After complete dissolution, the $SO_4^{2-}$ concentration does not drop like in the urban aerosol case, dispite the dilution of the salt solution with increasing relative humidity. This is because ammonia is in excess and buffers the solution, maintaining the pH and the sulfate/bisulfate ratio constant at a steady level. Finally, for RH=61.8% (deliquescence of ammonium nitrate), ISORROPIA and SEQUILIB agree in predicting the aerosol water content for the urban aerosol and remote continental cases. This is not the case for the non-urban aerosol, where ISORROPIA predicts a relatively small amount of water. This difference is from the different nitrate equilibrium constants, since nitrate mass at RH=61.8% as predicted by ISORROPIA is about half of SEQUILIB (Figure 7). However, the water content does not

follow a corresponding 1:2 ratio, because there is more ammonium sulfate dissolved in SEQUILIB (Figure 8) which absorbs an additional amount of water. After all the ammonium sulfate is dissolved at RH=68%, the water levels between SEQUILIB and ISORROPIA are in good agreement. The effect of dissolved ammonium sulfate on the water content can be seen in the steep slope of the water curve of ISORROPIA (Figure 6) between RH=61.8% and RH=68%, where the salt is rapidly dissolving (Figure 8).

The marine aerosol case is a sulfate poor, sodium rich system. As a result, the aerosol phase should consist primarily of sodium sulfate, sodium nitrate, sodium chloride and possibly ammonium nitrate and ammonium chloride. As shown in Table VI, a mixture of these four salts has a MDRH of 50%, while the minimum DRH of each component salt is DRH=61.8% (ammonium nitrate) (Table V). So, according to Equation (2), there is a mutual deliquescence region for relative humidities between 50% and 61.8%. In this aspect, the marine aerosol displays a behavior similar to the non-urban continental case. However, the dominating effect of sodium salts significantly changes the deliquescence behavior of the system. Figure 9 is a plot of predicted aerosol water content against relative humidity. For relative humidities below 50%, all models predict a solid aerosol (no water). When the RH reaches 50%, ISORROPIA predicts water, as a result of being in the mutual deliquescence region described above, while SEQUILIB and SCAPE predict only solids. For humidities greater than 61.8%, SEQUILIB calculates water from the deliquescence of ammonium nitrate, while SCAPE predicts significant aerosol water for relative humidities greater than 75.3%, the deliquescence point of sodium chloride. SEQUILIB predicts total dissolution of sodium chloride at RH=75.3% (just like SCAPE), while ISORROPIA predicts total dissolution of the salt at a lower value, RH=70%. This is seen in Figure 10, which plots the amount of solid sodium chloride in the aerosol phase as a function of relative humidity. By comparing Figure 9 and Figure 10, one can

clearly see that the water content of the aerosol is controlled mainly by the dissolved amount of sodium chloride, because the dissolution curves of the salt (Figure 10) follow the water curves exactly (Figure 9). After the deliquescence point of sodium chloride, all models predict the same water content.

Finally, Figure 11 shows a plot of total aerosol water per unit mass of aerosol salt as a function of relative humidity. Salt mass refers to the total amount of inorganic salts (dissolved and solid) that reside in the aerosol phase. ISORROPIA was used for the calculations. This plot shows the relative effectiveness of each aerosol type in absorbing water, since water is expressed on a per mass basis. This in turn can provide insight of the role each aerosol type might play in direct and indirect climate forcing. By examining Figure 11, for relative humidities between 50% and 60%, marine aerosol is marginally the most efficient water absorber. For relative humidities between 60% and about 67%, urban and remote continental aerosol dominate, while for relative humidities above 67 %, marine aerosol becomes the most efficient absorber of water. Thus generally speaking, marine aerosol is the most efficient water absorber of all four aerosol types examined.

The CPU time needed for each run is shown in Table VIII. ISORROPIA is clearly superior to both SCAPE and SEQUILIB, the speedup being at least an order of magnitude. On the other hand, the amount of time ISORROPIA required for each case was essentially constant, thus proving its capability for robust and rapid convergence. This type of behavior was not seen in the other two models, where the solution time varied considerably between cases.

## Summary and Conclusions

This paper presents a new equilibrium aerosol model, called ISORROPIA, which is comprehensive and computationally efficient. The model uses a weighted average approach to approximate the aerosol composition in mutual deliquescence regions, instead of performing the full calculations. This approximation reduces the necessary computations and is expected to speed up the solution time.

For internal consistency, ISORROPIA uses equilibrium constants and thermodynamic data obtained from a single source (Wagman *et al.*, 1982). The K-M method is used for calculating binary activity coefficients, while Bromley's rule is used for calculating the multicomponent activity coefficients. The ZSR method is used for calculating the aerosol water content, since it is easy to use and has comparable accuracy with other more rigorous algorithms (Kim *et al.*, 1993). The temperature dependence coefficients for all reactions and deliquescence relative humidities (single salt and multicomponent mixtures) are calculated and used. DRH values at 298.15K for single salts are obtained from Kim *et al.* (1993), while MDRH points are obtained from maps calculated by Potukuchi and Wexler (1995a, 1995b).

ISORROPIA was compared with SEQUILIB (Pilinis and Seinfeld, 1987) and SCAPE (Kim *et al.*, 1993) for four types of aerosol systems. The three models generally agree well in their predictions. Any differences between them were encountered mainly in low relative humidities, where the ionic strength of the aqueous solutions is very large. This is because the equilibrium point depends on activity coefficients, which are very sensitive to water changes. It becomes apparent that the most crucial part in the solution algorithm is the correct prediction of dissolved solids, since this significantly affects aerosol water content. A small perturbation in water can eventually lead to total dissolution or precipitation of a salt, especially for low relative humidities. Differences were also seen

in mutual deliquescence regions, where, in contrast to SCAPE and SEQUILIB, ISORROPIA predicted an aqueous phase. After comparing the water content per unit aerosol salt mass for all aerosol types, marine aerosol proved to be the most efficient in absorption of water over a significant range of relative humidities.

Finally, ISORROPIA is very fast, with CPU times at least an order of magnitude lower than the other models. Especially for the marine aerosol case, ISORROPIA was more than four hundred times faster than SCAPE and ten times faster than SEQUILIB. Apart from its speed, the model proved to be robust and fast in convergence, since roughly the same amount of CPU time was needed for all the cases examined.

## Acknowledgments

This research was conducted with support from the Environmental Protection Agency under grant R-824793010 and from the National Science Foundation under grant ATM-9625718. A.N. acknowledges the support of an ONR studentship by grant N000149510807.

## References

Allen, A.G., Harrison, R.M., Erisman, J.W. (1989) Field measurements of the dissociation of ammonium nitrate and ammonium chloride aerosols. *Atmos. Environ*., **23**, 1591-1599.

Bassett, M., and Seinfeld, J. H. (1983) Atmospheric equilibrium model of sulfate and nitrate aerosols. *Atmos. Environ*., **17**, 2237-2252.

Bassett, M., and Seinfeld, J. H. (1984) Atmospheric equilibrium model of sulfate and nitrate aerosols-II. Particle size analysis. *Atmos. Environ.*, **18**, 1163-1170.

Bromley, L.A. (1973) Thermodynamic properties of strong electrolytes in aqueous solutions. *AIChE J.*, **19**, 313-320.

Charlson, R.J., Lovelock, J.E., Andreae, M.O. and Warren, S.G. (1987) Oceanic phytoplankton, atmospheric sulphur, cloud albedo and climate. *Nature*, **326**, 655-661.

Denbeigh, K. (1981) *The principles of chemical equilibrium*. Fourth Ed., Cambridge University Press, Cambridge.

Deepak, A. and Gali, G. (1991) *The international global aerosol program (IGAP) plan*. Deepak Publishing, Hampton, Virginia.

Fitzgerald, J.W. (1991) Marine aerosols: A review. *Atmos. Environ*, **25A**, 533-545.

Heintzenberg, J. (1989) Fine particles in the global troposphere, A review.*Tellus*, **41B**, 149-160.

Hildemann, L.M., Russell, A.G. and Cass, G.R. (1984) Ammonia and nitric acid concentrations in equilibrium with atmospheric aerosols: Experiment vs. Theory. *Atmos. Environ.*, **18**, 1737-1750.

Jacobson, M.Z., Tabazadeh, A., Turco, R.P. (1996) Simulating equilibrium within aerosols and nonequilibrium between gases and aerosols. *J. Geophys. Res.*, **101**, 9079-9091.

Kim, Y.P., Seinfeld, J.H. and Saxena, P. (1993) Atmopsheric gas-aerosol equilibrium I. Thermodynamic model. *Aerosol Sci. Technol.*, **19**, 157-181.

Kim, Y.P., Seinfeld, J.H. and Saxena, P. (1993b) Atmopsheric gas-aerosol equilibrium II. Analysis of common approximations and activity coefficient methods. *Aerosol Sci. Technol.*, **19**, 182-198.

Kusik, C.L. and Meissner, H.P. (1978) Electrolyte activity coefficients in inorganic processing. *AIChE Symp. Series,* **173**, 14-20.

Meng, Z. and Seinfeld, J.H. (1996) Time scales to achieve atmospheric gas-aerosol equilibrium for volatile species. *Atmos. Environ.*, **30**, 2889-2900.

Pandis, S.N., Wexler, A.S., Seinfeld, J.H. (1995) Dynamics of tropospheric aerosols. *J. Phys. Chem.*, **99**, 9646-9659.

Pilinis, C. and Seinfeld, J.H. (1987) Continued development of a general equilibrium model for inorganic multicomponent atmospheric aerosols. *Atmos. Environ.* **21**, 2453-2466.

Pilinis, C., Pandis, S.N., Seinfeld, J.H. (1995) Sensitivity of direct climate forcing by atmospheric aerosols to aerosols size and composition. *J. Geophys. Res.*, **100**, 18739-18754.

Pitzer, K.S. and Mayorga, G. (1973) Thermodynamics of electrolytes - II. Activity and osmotic coefficients for strong electrolytes with one or both ions univalent. *J. Phys. Chem.*, **77**, 2300-2308.

Potukuchi, S. and Wexler, A.S. (1995a) Identifying solid-aqueous phase transitions in atmospheric aerosols - I. Neutral-acidity solutions. *Atmos. Environ.*, **29**, 1663-1676.

Potukuchi, S. and Wexler, A.S. (1995b) Identifying solid-aqueous phase transitions in atmospheric aerosols - II. Acidic solutions. *Atmos. Environ.*, **29**, 3357-3364.

Quinn, P.K., Asher, W.E. and Charlson R.J. (1992) Equilibria of the marine multiphase ammonia system. *J. Atmos. Chem.*, **14**, 11-30.

Robinson, R.A. and Stokes, R.H. (1965) *Electrolyte solutions*. Second Ed., Butterworths, London.

Russell, L.M., Pandis, S.N., Seinfeld, J.H. (1994) Aerosol production and growth in the marine boundary layer. *J. Geophys. Res.*, **99**, 20989-21003.

Saxena, P. and Peterson, T.W. (1981) Thermodynamics of multicomponent electrolytic aerosols. *J. Coll. Interf. Sci.*, **79**, 496-510.

Saxena, P., Hudischewsky, A.B., Seigneur, C., Seinfeld, J.H. (1986) A comparative study of equilibrium approaches to the chemical characterization of secondary aerosols. *Atmos. Environ.*, **20**, 1471-1483.

Saxena, P., Mueller, P.K., Kim, Y.P., Seinfeld, J.H., Koutrakis, P. (1993) Coupling thermodynamic theory with measurments to characterize acidity of atmospheric aerosols. *Aeros. Sci. Tech*., **19**, 279-293.

Tang, I.N. and Munkelwitz, H.R. (1993) Composition and temperature dependance of the deliquescence properties of hygroscopic aerosols. *Atmos. Environ.*, **27A**, 467-473.

Wagman, D.D., Evans, W.H., Parker, V.B., Schumm, R.H., Harlow, I., Bailey, S.M., Churney, K.L., Nuttall, R.L. (1982) The NBS tables of chemical thermodynamic properties. *J. Phys. Chem. Ref. Data*. Vol. 11, Suppl. 2

Wexler, A.S. and Seinfeld, J.H. (1991) Second-generation inorganic aerosol model. *Atmos. Environ.* **25A**, 2731-2748.

Table I: Equilibrium Relations and Constants [*]

| Reaction | Constant expression | K° (298.15K) | $\frac{\Delta H^o(T_o)}{RT_o}$ | $\frac{\Delta C_p^o}{R}$ | Units |
|---|---|---|---|---|---|
| $HSO_{4(aq)}^- \xleftrightarrow{K_1} H_{(aq)}^+ + SO_{4(aq)}^{2-}$ | $\frac{[H^+][SO_4^{2-}]}{[HSO_4^-]}\frac{\gamma_{H^+}\gamma_{SO_4^{2-}}}{\gamma_{HSO_4^-}}$ | $1.015\times10^{-2}$ | 8.85 | 25.14 | mol kg$^{-1}$ |
| $NH_{3(g)} \xleftrightarrow{K_{21}} NH_{3(aq)}$ | $\frac{[NH_{3(aq)}]}{[P_{NH_3}]}\gamma_{NH_3}$ | $5.764\times10^{1}$ | 13.79 | -5.39 | mol kg$^{-1}$ atm$^{-1}$ |
| $NH_{3(aq)} + H_2O_{(aq)} \xleftrightarrow{K_{22}} NH_{4(aq)}^+ + OH_{(aq)}^-$ | $\frac{[NH_4^+][OH^-]}{[NH_{3(aq)}]a_w}\frac{\gamma_{NH_4^+}\gamma_{OH^-}}{\gamma_{NH_3}}$ | $1.805\times10^{-5}$ | -1.50 | 26.92 | mol kg$^{-1}$ |
| $HNO_{3(g)} \xleftrightarrow{K_4} H_{(aq)}^+ + NO_{3(aq)}^-$ | $\frac{[H^+][NO_3^-]}{P_{HNO_3}}\gamma_{H^+}\gamma_{NO_3^-}$ | $2.511\times10^{6}$ | 29.17 | 16.83 | mol$^2$ kg$^{-2}$ atm$^{-1}$ |
| $HCl_{(g)} \xleftrightarrow{K_3} H_{(aq)}^+ + Cl_{(aq)}^-$ | $\frac{[H^+][Cl^-]}{P_{HCl}}\gamma_{H^+}\gamma_{Cl^-}$ | $1.971\times10^{6}$ | 30.20 | 19.91 | mol$^2$ kg$^{-2}$ atm$^{-1}$ |
| $H_2O_{(aq)} \xleftrightarrow{K_w} H_{(aq)}^+ + OH_{(aq)}^-$ | $\frac{[H^+][OH^-]}{a_w}\gamma_{H^+}\gamma_{OH^-}$ | $1.010\times10^{-14}$ | -22.52 | 26.92 | mol$^2$ kg$^{-2}$ |
| $Na_2SO_{4(s)} \xleftrightarrow{K_5} 2Na_{(aq)}^+ + SO_{4(aq)}^{2-}$ | $[Na^+]^2[SO_4^{2-}]\gamma_{Na^+}^2\gamma_{SO_4^{2-}}$ | $4.799\times10^{-1}$ | 0.98 | 39.75 | mol$^3$ kg$^{-3}$ |
| $(NH_4)_2SO_{4(s)} \xleftrightarrow{K_7} 2NH_{4(aq)}^+ + SO_{4(aq)}^{2-}$ | $[NH_4^+]^2[SO_4^{2-}]\gamma_{NH_4^+}^2\gamma_{SO_4^{2-}}$ | $1.817\times10^{0}$ | -2.65 | 38.57 | mol$^3$ kg$^{-3}$ |
| $NH_4Cl_{(s)} \xleftrightarrow{K_6} NH_{3(g)} + HCl_{(g)}$ | $P_{NH_3}P_{HCl}$ | $1.086\times10^{-16}$ | -71.00 | 2.40 | atm$^2$ |
| $NaNO_{3(s)} \xleftrightarrow{K_9} Na_{(aq)}^+ + NO_{3(aq)}^-$ | $[Na^+][NO_3^-]\gamma_{Na^+}\gamma_{NO_3^-}$ | $1.197\times10^{1}$ | -8.22 | 16.01 | mol$^2$ kg$^{-2}$ |
| $NaCl_{(s)} \xleftrightarrow{K_8} Na_{(aq)}^+ + Cl_{(aq)}^-$ | $[Na^+][Cl^-]\gamma_{Na^+}\gamma_{Cl^-}$ | $3.766\times10^{1}$ | -1.56 | 16.90 | mol$^2$ kg$^{-2}$ |
| $NaHSO_{4(s)} \xleftrightarrow{K_{11}} Na_{(aq)}^+ + HSO_{4(aq)}^-$ | $[Na^+][HSO_4^-]\gamma_{Na^+}\gamma_{HSO_4^-}$ | $2.413\times10^{4}$ | 0.79 | 14.75 | mol$^2$ kg$^{-2}$ |
| $NH_4NO_{3(s)} \xleftrightarrow{K_{10}} NH_{3(g)} + HNO_{3(g)}$ | $P_{NH_3}P_{HNO_3}$ | $5.746\times10^{-17}$ | -74.38 | 6.12 | atm$^2$ |
| $NH_4HSO_{4(s)} \xleftrightarrow{K_{12}} NH_{4(aq)}^+ + HSO_{4(aq)}^-$ | $[NH_4^+][HSO_4^-]\gamma_{NH_4^+}\gamma_{HSO_4^-}$ | $1.383\times10^{0}$ | -2.87 | 15.83 | mol$^2$ kg$^{-2}$ |
| $(NH_4)_3H(SO_4)_{2(s)} \xleftrightarrow{K_{13}} 3NH_{4(aq)}^+ + HSO_{4(aq)}^- + SO_{4(aq)}^{2-}$ | $[NH_4^+]^3[SO_4^{2-}][HSO_4^-]\times\gamma_{NH_4^+}^3\gamma_{SO_4^{2-}}\gamma_{HSO_4^-}$ | $2.972\times10^{1}$ | -5.19 | 54.40 | mol$^5$ kg$^{-5}$ |

[*] source: Kim *et al.*, (1993)

Table II: Thermodynamic Properties for species in ISORROPIA*

| Species | $\Delta G_f^o$ (kJ mol$^{-1}$) | $\Delta H_f^o$ (kJ mol$^{-1}$) | $C_p^o$ (J mol$^{-1}$ K$^{-1}$) |
|---|---|---|---|
| $NaCl_{(s)}$ | -384.138 | -411.153 | 50.500 |
| $NaNO_{3\,(s)}$ | -367.000 | -467.850 | 92.880 |
| $Na_2SO_{4\,(s)}$ | -1270.160 | -1387.080 | 128.200 |
| $NaHSO_{4\,(s)}$ | -992.800 | -1125.500 | 85.000 |
| $NH_4Cl_{\,(s)}$ | -202.870 | -314.430 | 84.100 |
| $NH_4NO_{3\,(s)}$ | -183.870 | -365.560 | 139.300 |
| $(NH_4)_2SO_{4\,(s)}$ | -901.670 | -1180.850 | 187.490 |
| $NH_4HSO_{4\,(s)}$ | -823.000 | -1026.960 | 127.500 |
| $(NH_4)_3H(SO_4)_{2\,(s)}$ | -1730.000 | -2207.000 | 315.000 |
| $HNO_{3\,(g)}$ | -74.720 | -135.060 | 53.350 |
| $HCl_{\,(g)}$ | -95.299 | -92.307 | 29.126 |
| $NH_{3\,(g)}$ | -16.450 | -46.110 | 35.060 |
| $H^+_{\,(aq)}$ | 0.000 | 0.000 | 0.000 |
| $Na^+_{\,(aq)}$ | -261.905 | -240.120 | 46.400 |
| $NH_4^+{}_{(aq)}$ | -79.310 | -132.510 | 79.900 |
| $HSO_4^-{}_{(aq)}$ | -755.910 | -887.340 | -84.000 |
| $SO_4^{2-}{}_{(aq)}$ | -744.530 | -909.270 | -293.000 |
| $NO_3^-{}_{(aq)}$ | -111.250 | -207.360 | -86.600 |
| $Cl^-_{(aq)}$ | -131.228 | -167.159 | -136.400 |
| $OH^-_{(aq)}$ | -157.244 | -229.994 | -148.500 |

* source: Kim *et al.*, (1993)

Table III: Possible species for the four basic aerosol types.

| Sulfate Ratio | Sodium Ratio | Aerosol Type | Solid Species | Ions | Gases |
|---|---|---|---|---|---|
| $R_{SO_4} < 1$ | any value | Sulfate Rich (very acidic) | $NaHSO_4$ $NH_4HSO_4$ | $Na^+$, $NH_4^+$, $H^+$, $HSO4^-$, $SO_4^{2-}$, $NO_3^-$, $Cl^-$, $H_2O$ | $HNO_3$, HCl, $H_2O$ |
| $1 \leq R_{SO_4} < 2$ | any value | Sulfate Rich | $NaHSO_4$ $NH_4HSO_4$ $Na_2SO_4$ $(NH_4)_2SO_4$ $(NH_4)_3H(SO_4)_2$ | $Na^+$, $NH_4^+$, $H^+$, $HSO4^-$, $SO_4^{2-}$, $NO_3^-$, $Cl^-$, $H_2O$ | $HNO_3$, HCl, $H_2O$ |
| $R_{SO_4} \geq 2$ | $R_{Na} < 2$ | Sulfate Poor Sodium Poor | $Na_2SO_4$ $(NH_4)_2SO_4$ $NH_4NO_3$ $NH_4Cl$ | $Na^+$, $NH_4^+$, $H^+$, $HSO4^-$, $SO_4^{2-}$, $NO_3^-$, $Cl^-$, $H_2O$ | $HNO_3$, HCl, $NH_3$, $H_2O$ |
| $R_{SO_4} \geq 2$ | $R_{Na} \geq 2$ | Sulfate Poor Sodium Rich | $Na_2SO_4$ $NaNO_3$ NaCl $NH_4NO_3$ $NH_4Cl$ | $Na^+$, $NH_4^+$, $H^+$, $HSO4^-$, $SO_4^{2-}$, $NO_3^-$, $Cl^-$, $H_2O$ | $HNO_3$, HCl, $NH_3$, $H_2O$ |

Table IV: Kusik-Meissner parameters for the species used in ISORROPIA*

| Species | q |
|---|---|
| NaCl | 2.23 |
| $Na_2SO_4$ | -0.19 |
| $NaNO_3$ | -0.39 |
| $(NH_4)_2SO_4$ | -0.25 |
| $NH_4NO_3$ | -1.15 |
| $NH_4Cl$ | 0.82 |
| $H_2SO_4$ | 0.70 |
| $H\text{-}HSO_4$ | 8.00 |
| $NH_4HSO_4$ | - |
| $HNO_3$ | 2.60 |
| HCl | 6.00 |
| $NaHSO_4$ | - |
| $(NH_4)_3H(SO_4)_2$ | - |

* source: Kim *et al.*, (1993)

Table V: Deliquescence relative humidities and temperature dependence of all salts modeled in ISORROPIA*

| Salt | DRH (298.15 K) | $-\frac{18}{1000R}L_s m_s$ |
|---|---|---|
| NaCl | 0.7528 | 25.0 |
| $Na_2SO_4$ | 0.9300 | 80.0 |
| $NaNO_3$ | 0.7379 | 304.0 |
| $(NH_4)_2SO_4$ | 0.7997 | 80.0 |
| $NH_4NO_3$ | 0.6183 | 852.0 |
| $NH_4Cl$ | 0.7710 | 239.0 |
| $NH_4HSO_4$ | 0.4000 | 384.0 |
| $NaHSO_4$ | 0.5200 | -45.0 |
| $(NH_4)_3H(SO_4)_2$ | 0.6900 | 186.0 |

* source: Kim *et al.*, (1993)

Table VI: Mutual deliquescence relative humidities and temperature dependence factors

| Salt Mixture | MDRH* (298.15 K) | $-\frac{18}{1000R}\sum_i L_{si}m_{si}$ |
|---|---|---|
| $NH_4NO_3$, $(NH_4)_2SO_4$ | 0.600 | 932 |
| $NH_4NO_3$, $(NH_4)_2SO_4$, $Na_2SO_4$, $NH_4Cl$ | 0.500 | 3951 |
| $(NH_4)_2SO_4$, $Na_2SO_4$, $NH_4Cl$ | 0.540 | 71 |
| $(NH_4)_2SO_4$, $Na_2SO_4$ | 0.760 | 71 |
| $NH_4NO_3$, $NH_4Cl$, $Na_2SO_4$, NaCl, $NaNO_3$ | 0.500 | 3951 |
| $NH_4Cl$, $Na_2SO_4$, NaCl, $NaNO_3$ | 0.540 | 2306 |
| $(NH_4)_3H(SO_4)_2$ , $NaHSO_4$, $Na_2SO_4$, $(NH_4)_2SO_4$ | 0.360 | 3951 |
| $(NH_4)_3H(SO_4)_2$ , $Na_2SO_4$, $(NH_4)_2SO_4$ | 0.675 | 2306 |
| $(NH_4)_3H(SO_4)_2$ , $NH_4HSO_4$ | 0.360 | 561 |
| $(NH_4)_3H(SO_4)_2$ , $(NH_4)_2SO_4$ | 0.675 | 262 |

* source: Potukuchi and Wexler, (1995a, 1995b)

Table VII: Aerosol types used in test case calculations

| | Concentrations ($\mu g\ m^{-3}$) | | | | | Ratios | |
|---|---|---|---|---|---|---|---|
| Aerosol type | Na | $NH_3$ | $H_2SO_4$ | $HNO_3$ | HCl | Sulfate | Sodium |
| Remote continental | 0.000 | 4.250 | 11.270 | 0.145 | 0.000 | 2.2 | 0.00 |
| Non-urban continental | 0.023 | 20.400 | 5.664 | 0.611 | 0.037 | 20.7 | 0.02 |
| Urban | 0.000 | 3.400 | 9.143 | 1.953 | 0.000 | 2.1 | 0.00 |
| Marine | 1.967 | 0.020 | 0.510 | 0.163 | 3.121 | 16.6 | 16.4 |

Table VIII: Absolute and relative execution times for all the aerosol cases tested.

| | ISORROPIA | SCAPE | | SEQUILIB | |
|---|---|---|---|---|---|
| Aerosol type | CPU time (sec) | CPU time(sec) | $\frac{t_{SCAPE}}{t_{ISORROPIA}}$ | CPU time(sec) | $\frac{t_{SEQUILIB}}{t_{ISORROPIA}}$ |
| Remote continental | 0.03 | 0.34 | 11.3 | 0.49 | 16.3 |
| Non-urban continental | 0.03 | 6.39 | 213.0 | 0.72 | 24.0 |
| Urban | 0.03 | 0.34 | 11.3 | 0.48 | 16.0 |
| Marine | 0.04 | 17.65 | 441.2 | 0.57 | 14.2 |

## Figure Captions

Figure 1: Aerosol water content (μg $m^{-3}$) as a function of relative humidity for the urban aerosol case.

Figure 2: Total aerosol nitrate (μg $m^{-3}$) as a function of relative humidity for the urban aerosol case.

Figure 3: Aqueous sulfate ($SO_4^{2-}$) (μg $m^{-3}$) as a function of relative humidity for the urban aerosol case.

Figure 4: Aerosol water content (μg $m^{-3}$) as a function of relative humidity for the remote continental aerosol case.

Figure 5: Total aerosol nitrate (μg $m^{-3}$) as a function of relative humidity for the remote continental aerosol case.

Figure 6: Aerosol water content (μg $m^{-3}$) as a function of relative humidity for the non-urban continental aerosol case.

Figure 7: Total aerosol nitrate (μg $m^{-3}$) as a function of relative humidity for the non-urban continental aerosol case.

Figure 8: Aqueous sulfate ($SO_4^{2-}$) (μg $m^{-3}$) as a function of relative humidity for the non-urban continental aerosol case.

Figure 9: Aerosol water content (μg $m^{-3}$) as a function of relative humidity for the marine aerosol case.

Figure 10: Solid sodium chloride (μg $m^{-3}$) as a function of relative humidity for the marine aerosol case.

Figure 11: Aerosol water per unit mass of aerosol salt as a function of relative humidity for all the aerosol cases. ISORROPIA was used for the calculations.

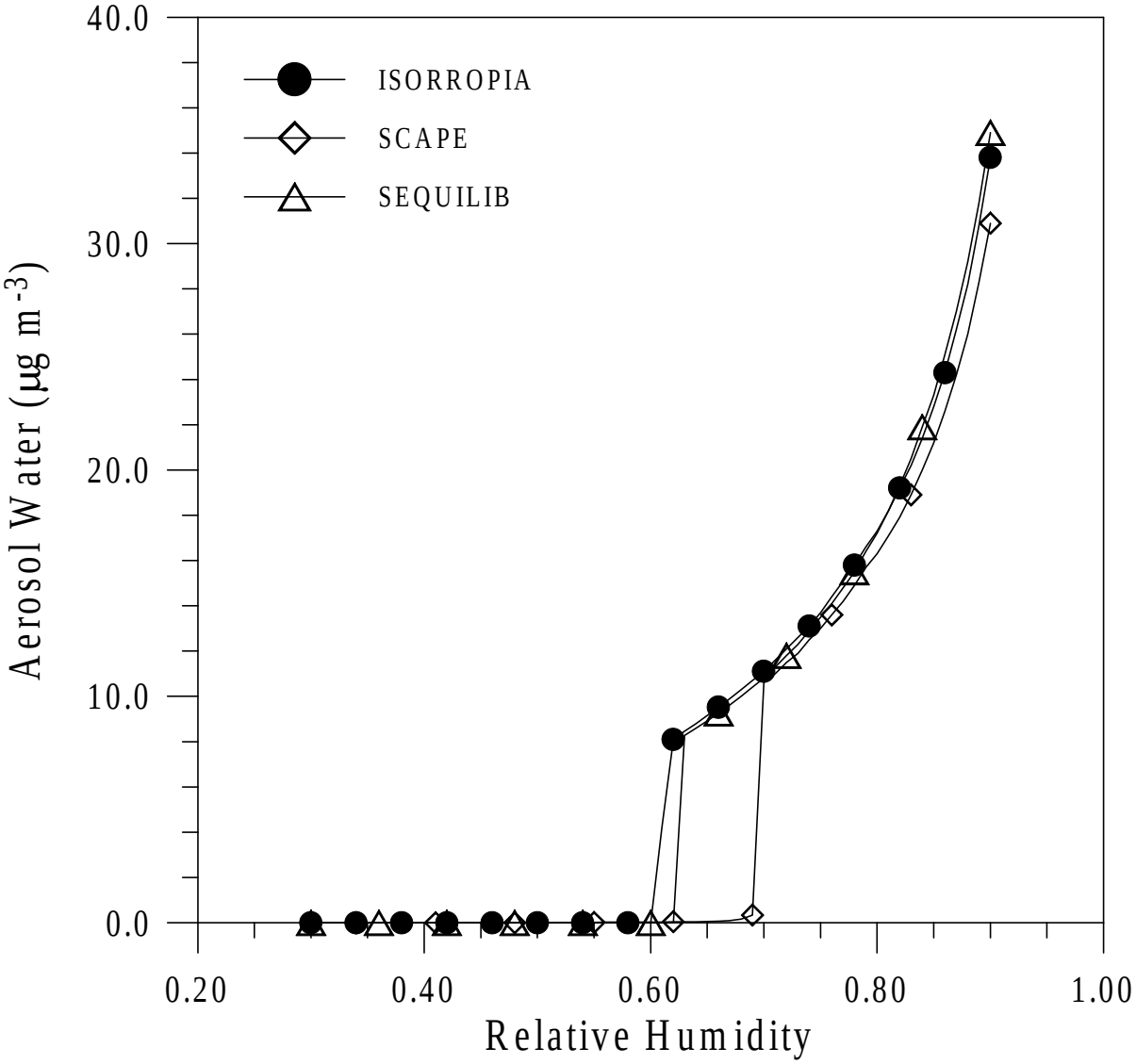
40.0
30.0
20.0
10.0
0.0
ISORROPIA
SCAPE
SEQUILIB
Aerosol Water (μg m-3)
0.20
0.40
0.60
0.80
1.00
Relative Humidity

Figure 1

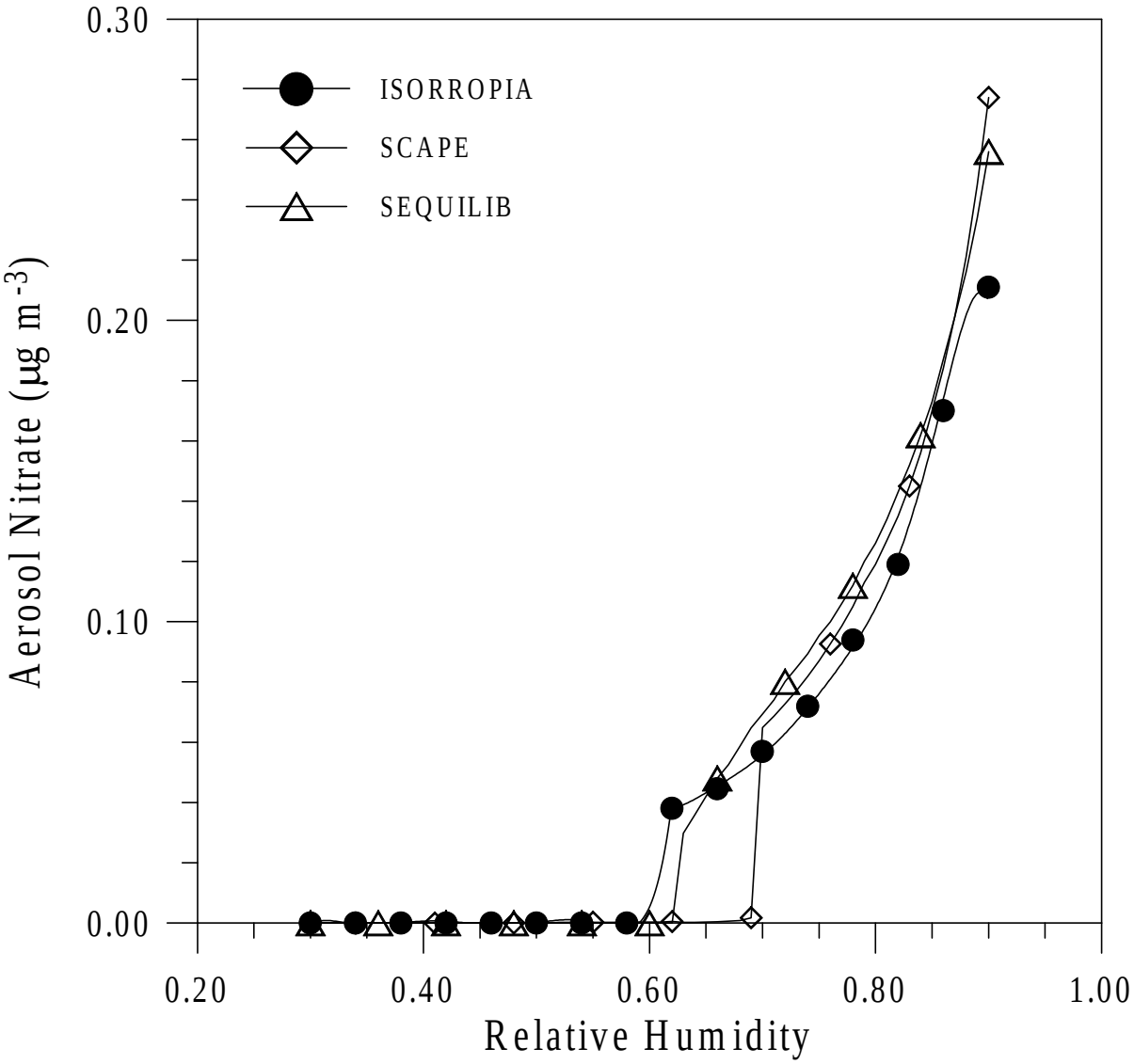
0.30
0.20
0.10
0.00
0.20
0.40
0.60
0.80
1.00
Relative Humidity
Aerosol Nitrate (μg m-3)
ISORROPIA
SCAPE
SEQUILIB

Figure 2

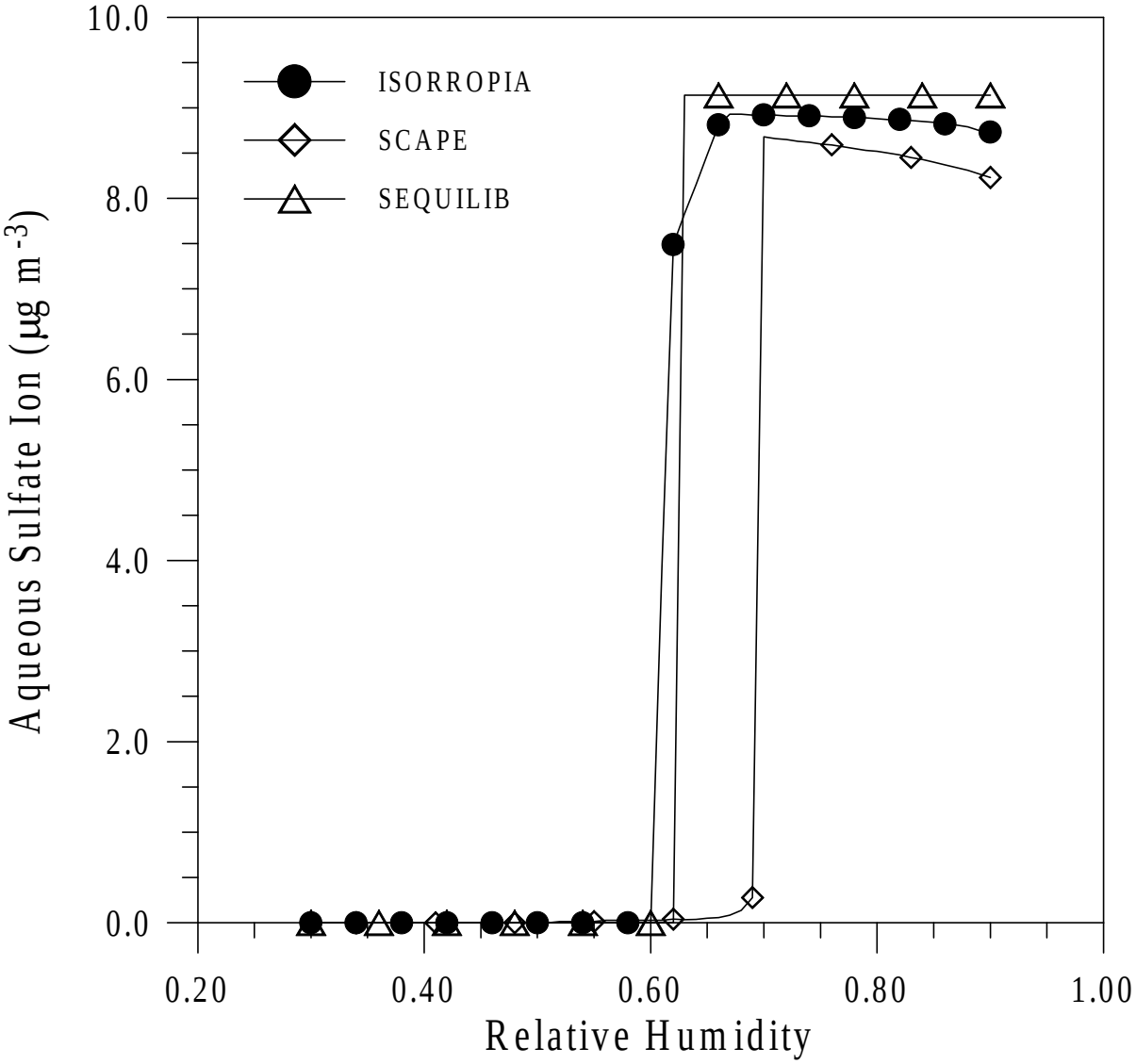
10.0
8.0
6.0
4.0
2.0
0.0
0.20
0.40
0.60
0.80
1.00
Aqueous Sulfate Ion (μg m-3)
Relative Humidity
ISORROPIA
SCAPE
SEQUILIB

Figure 3

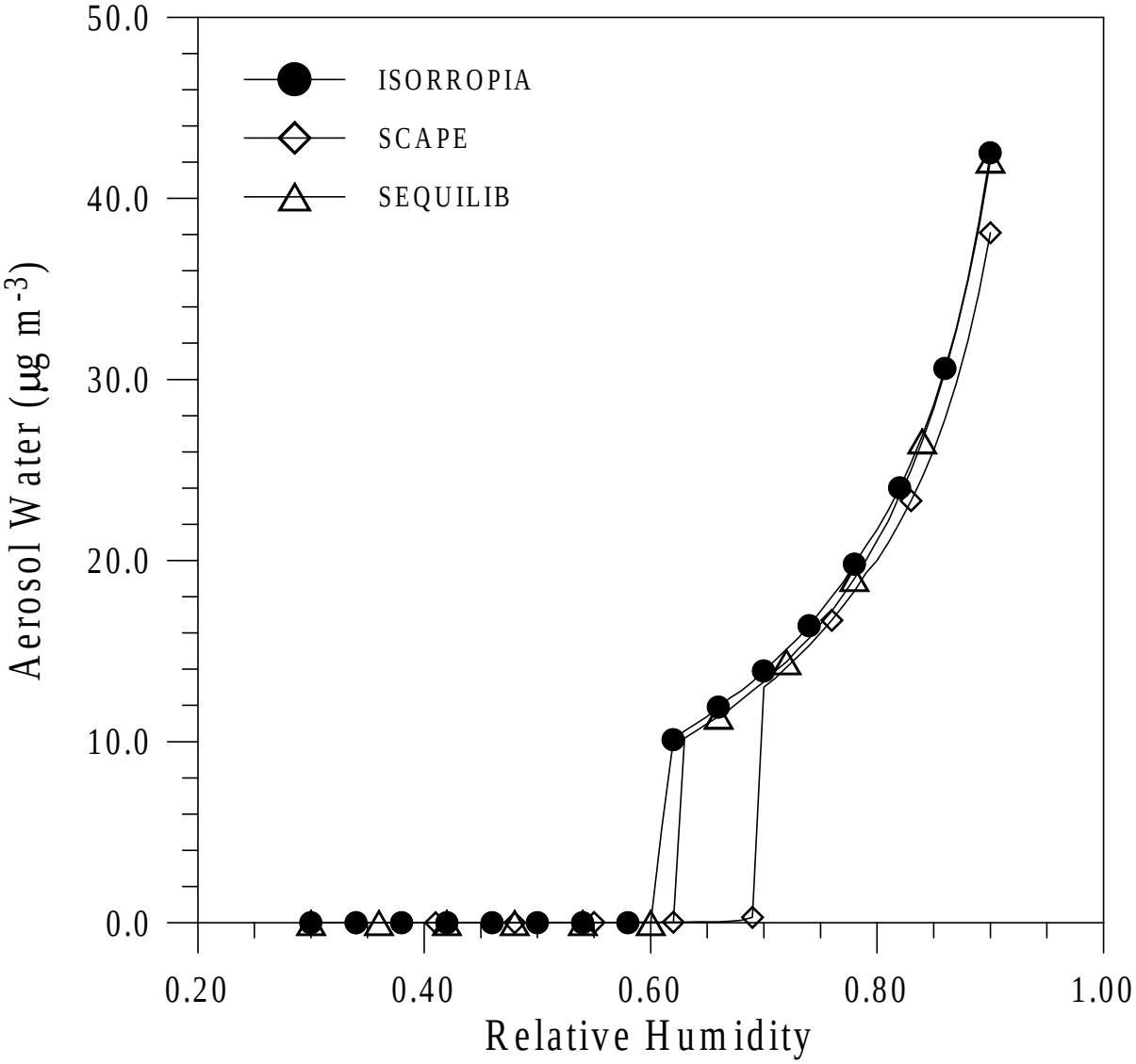
ISORROPIA
SCAPE
SEQUILIB
Aerosol Water (μg m-3)
50.0
40.0
30.0
20.0
10.0
0.0
0.20
0.40
0.60
0.80
1.00
Relative Humidity

Figure 4

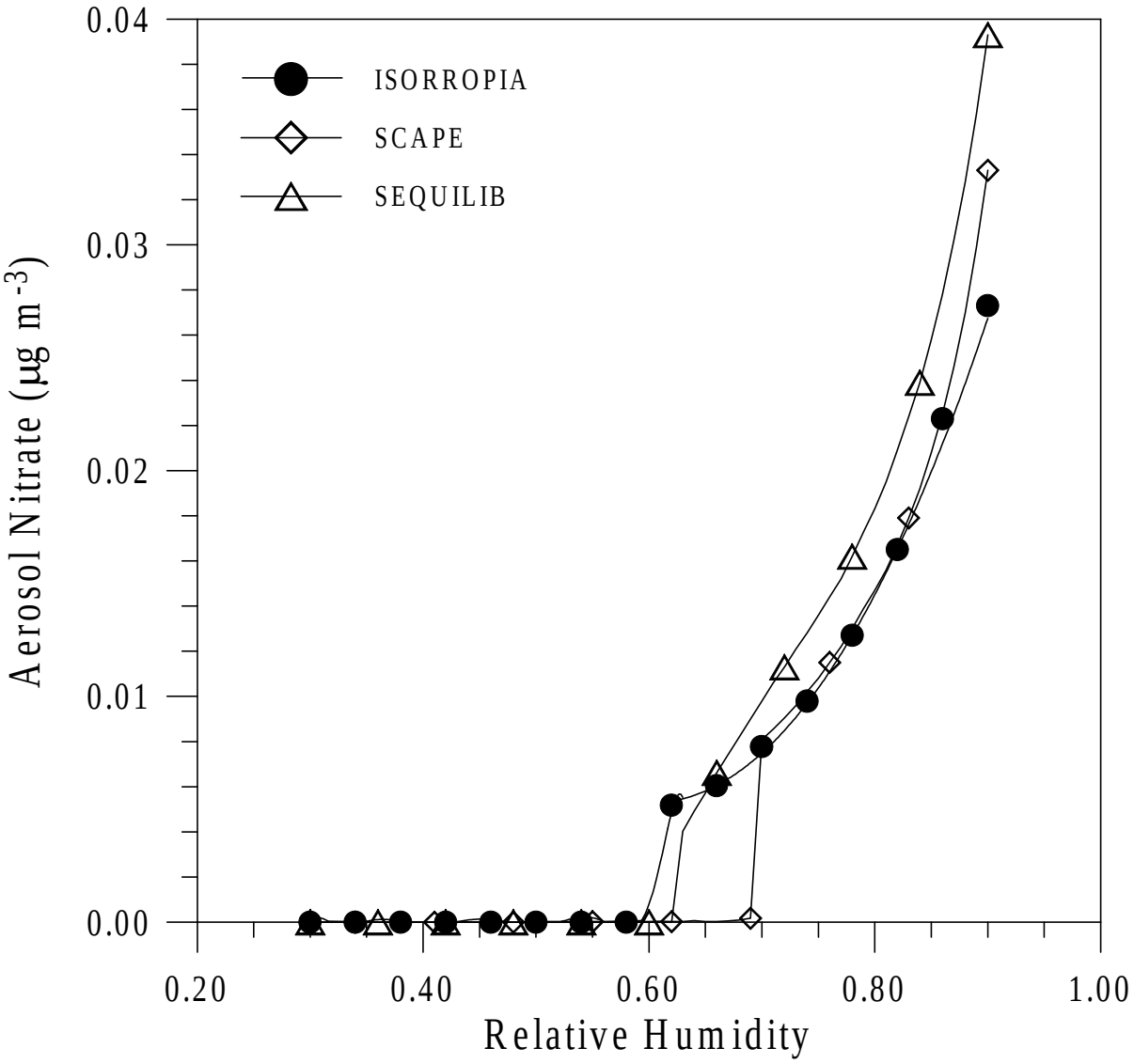
0.04
0.03
0.02
0.01
0.00
Aerosol Nitrate (μg m-3)
ISORROPIA
SCAPE
SEQUILIB
0.20
0.40
0.60
0.80
1.00
Relative Humidity

Figure 5

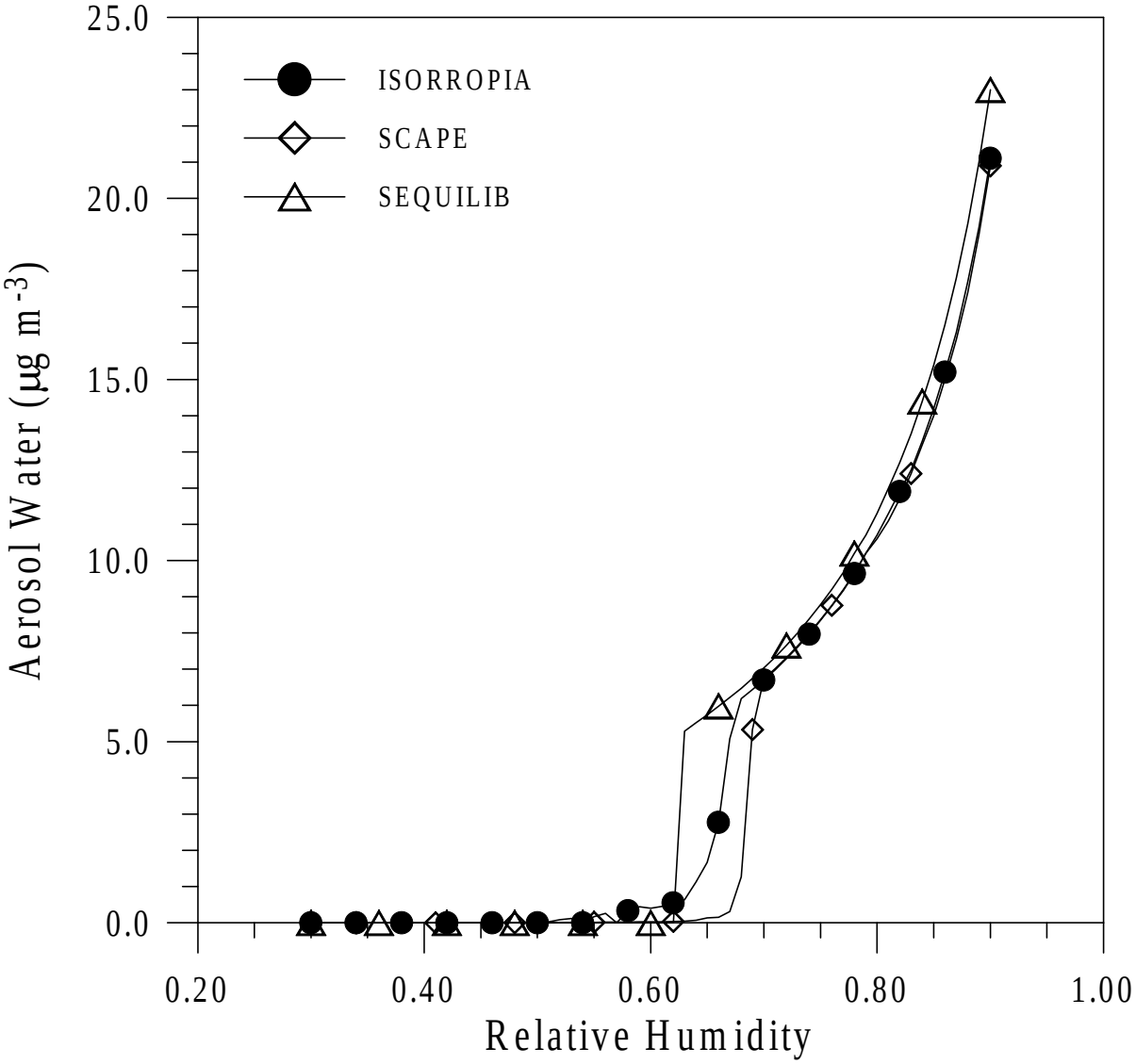
25.0
20.0
15.0
10.0
5.0
0.0
Aerosol Water (μg m-3)
ISORROPIA
SCAPE
SEQUILIB
0.20
0.40
0.60
0.80
1.00
Relative Humidity

Figure 6

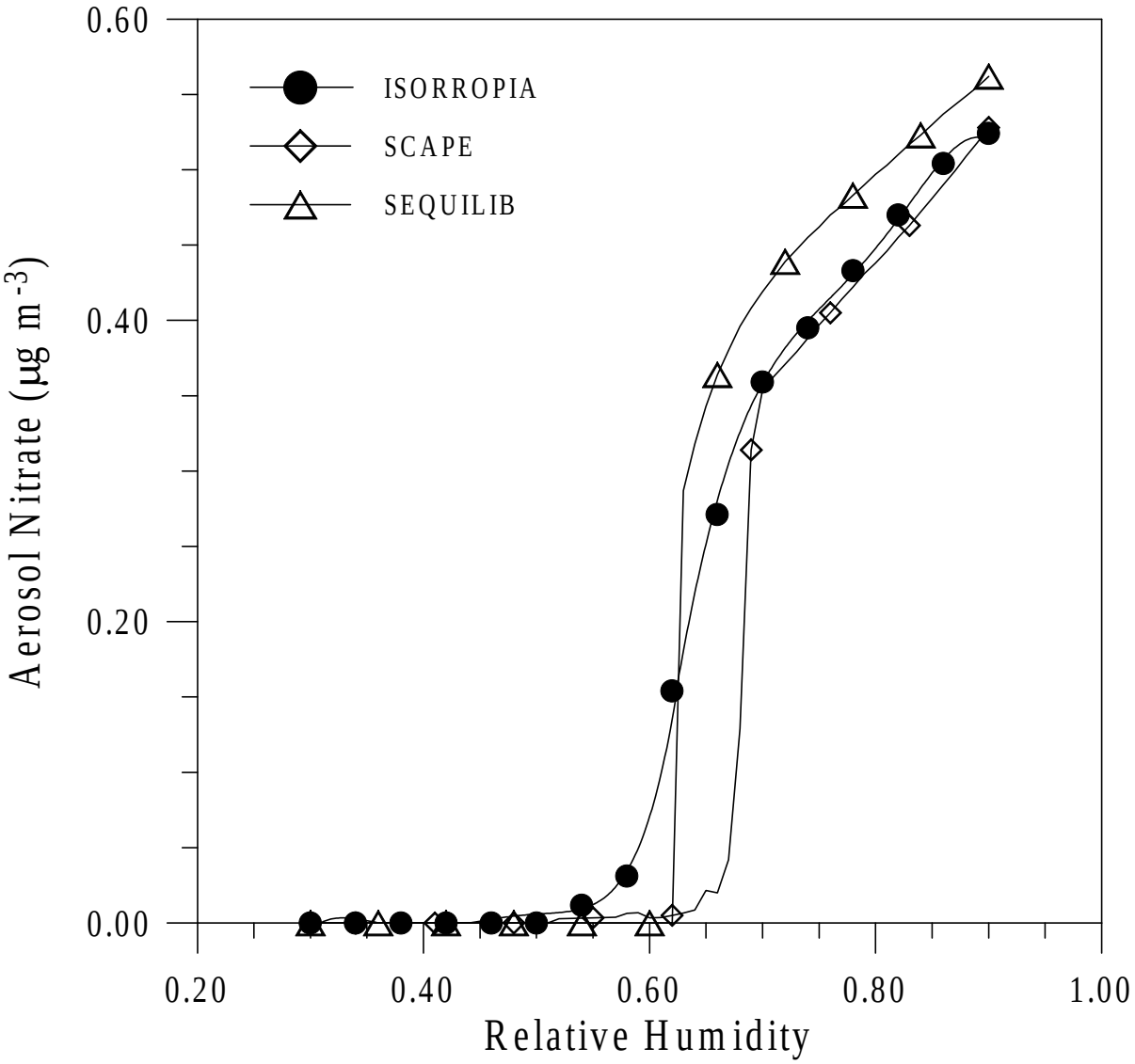
ISORROPIA
SCAPE
SEQUILIB
Aerosol Nitrate (μg m-3)
0.00
0.20
0.40
0.60
0.20
0.40
0.60
0.80
1.00
Relative Humidity

Figure 7

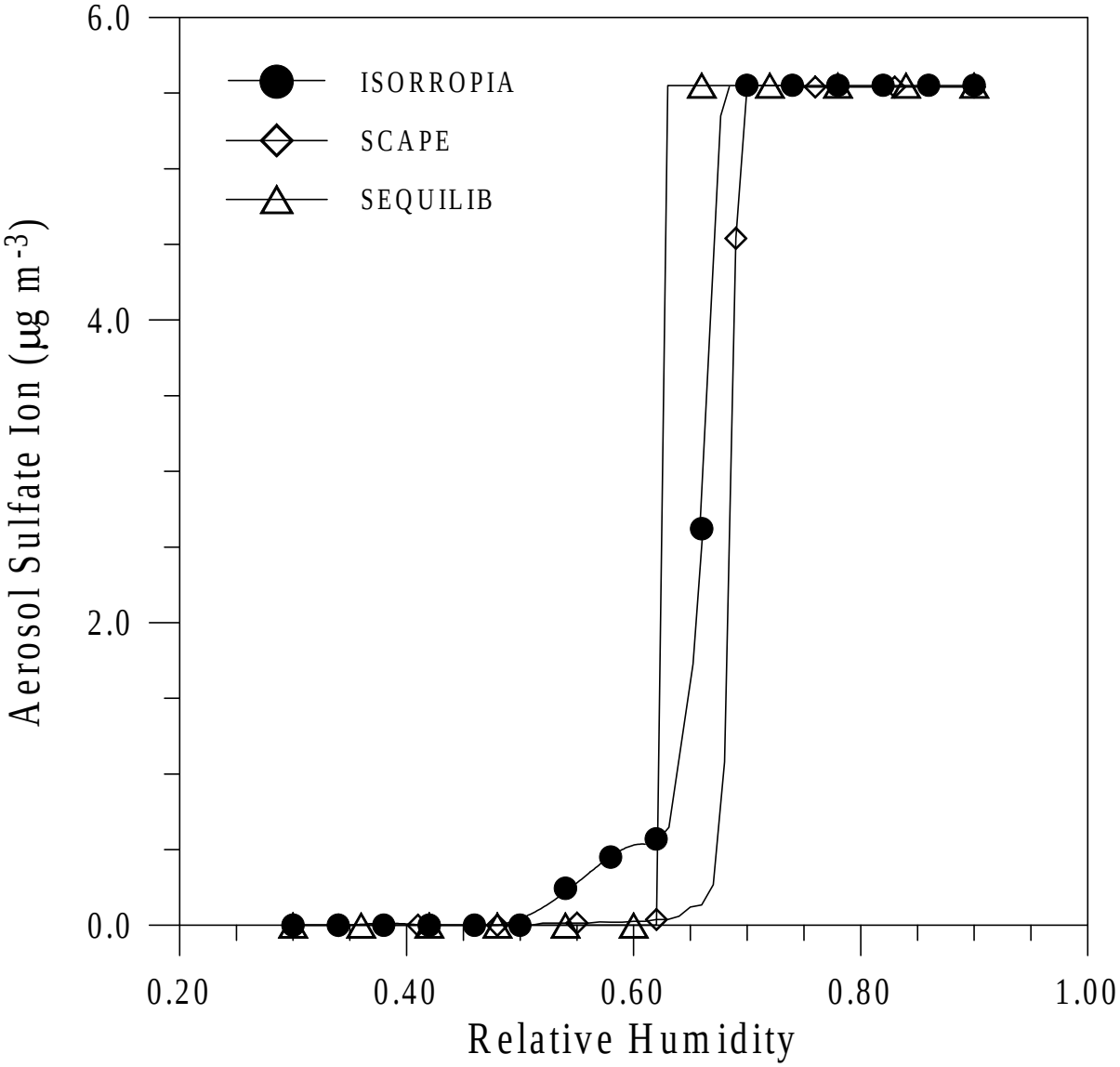
6.0
4.0
2.0
0.0
ISORROPIA
SCAPE
SEQUILIB
Aerosol Sulfate Ion (μg m-3)
0.20
0.40
0.60
0.80
1.00
Relative Humidity

Figure 8

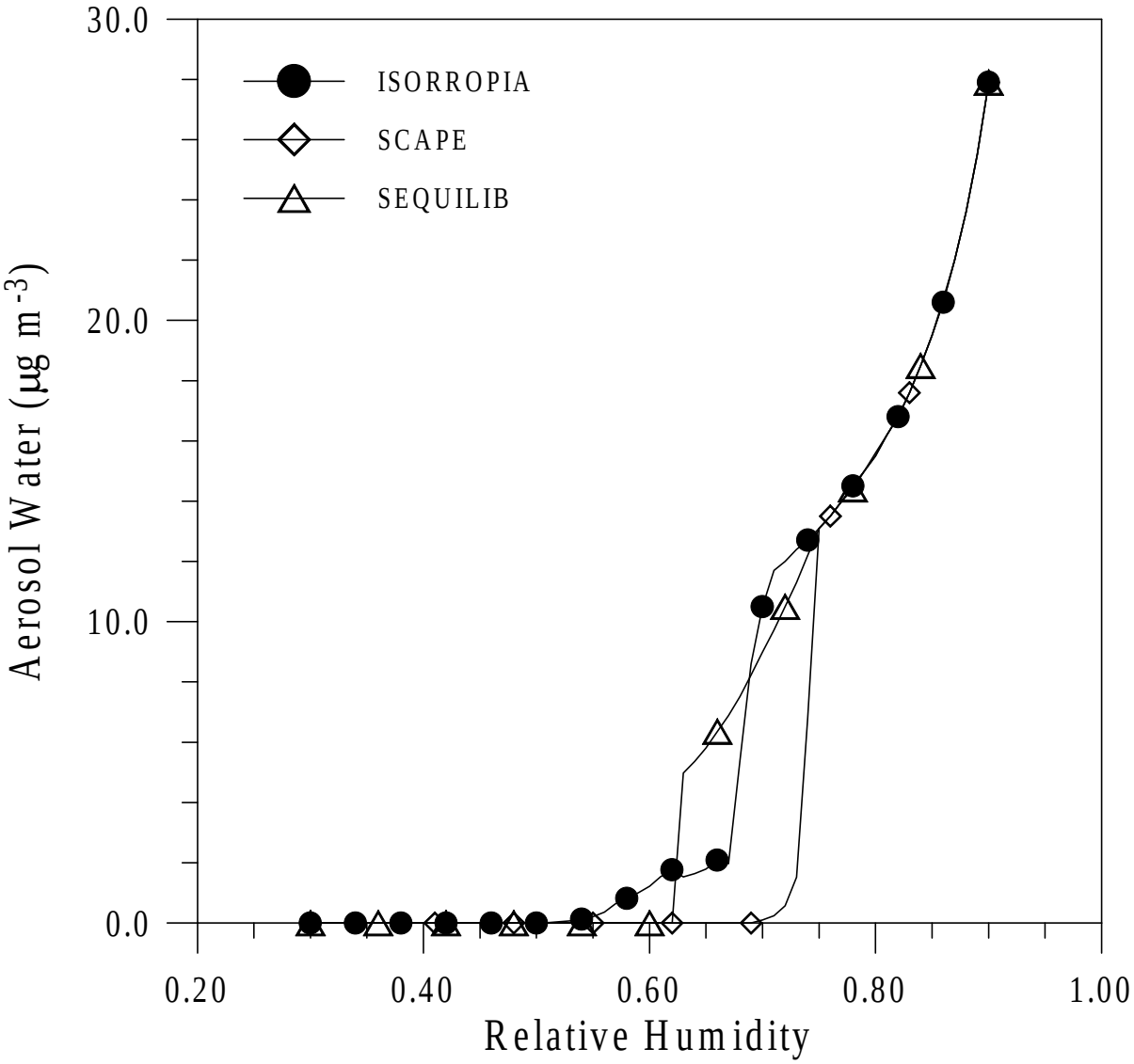
30.0
20.0
10.0
0.0
Aerosol Water (μg m-3)
ISORROPIA
SCAPE
SEQUILIB
0.20
0.40
0.60
0.80
1.00
Relative Humidity

Figure 9

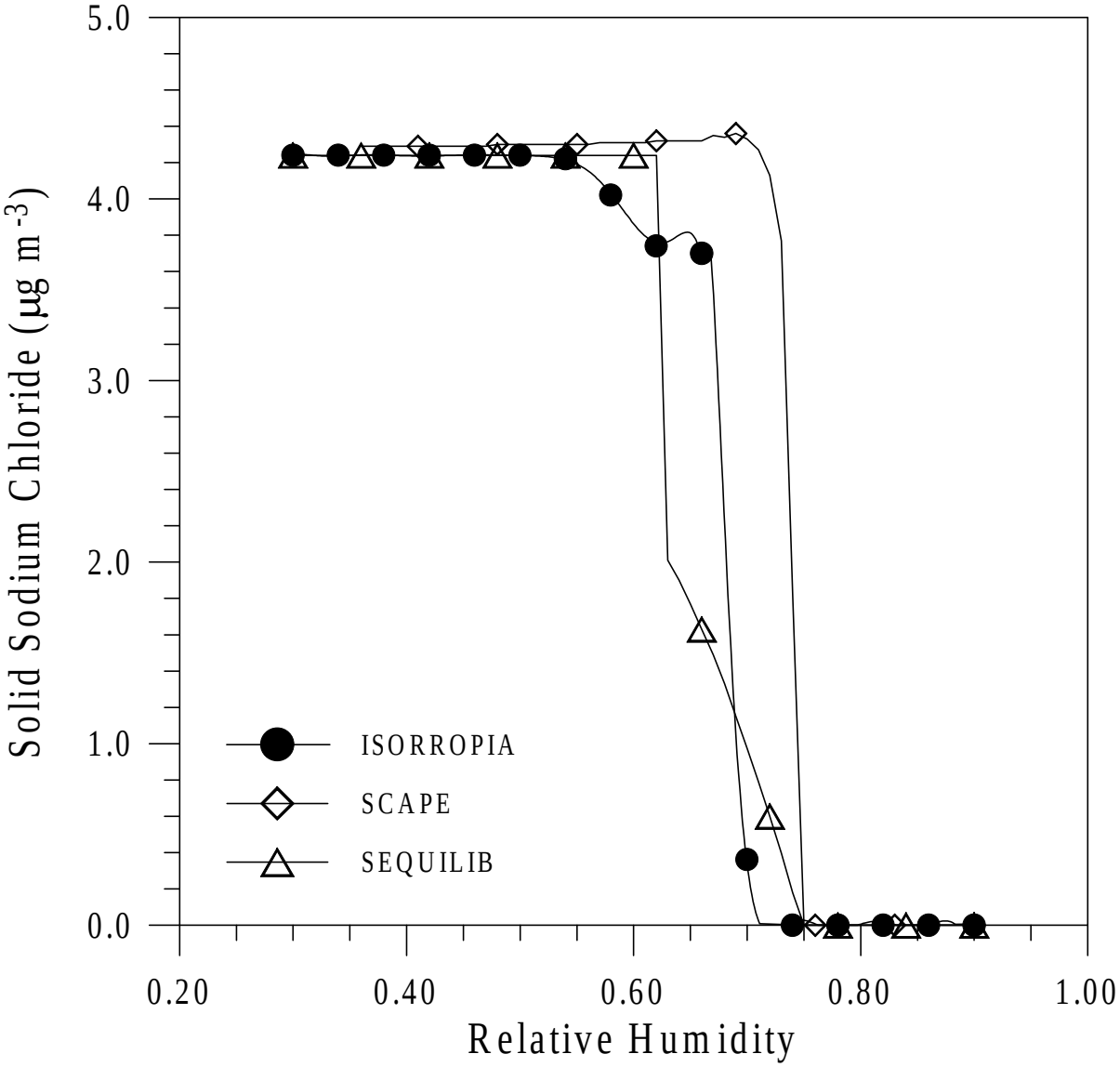
5.0
4.0
3.0
2.0
1.0
0.0
Solid Sodium Chloride (μg m-3)
0.20
0.40
0.60
0.80
1.00
Relative Humidity
ISORROPIA
SCAPE
SEQUILIB

Figure 10

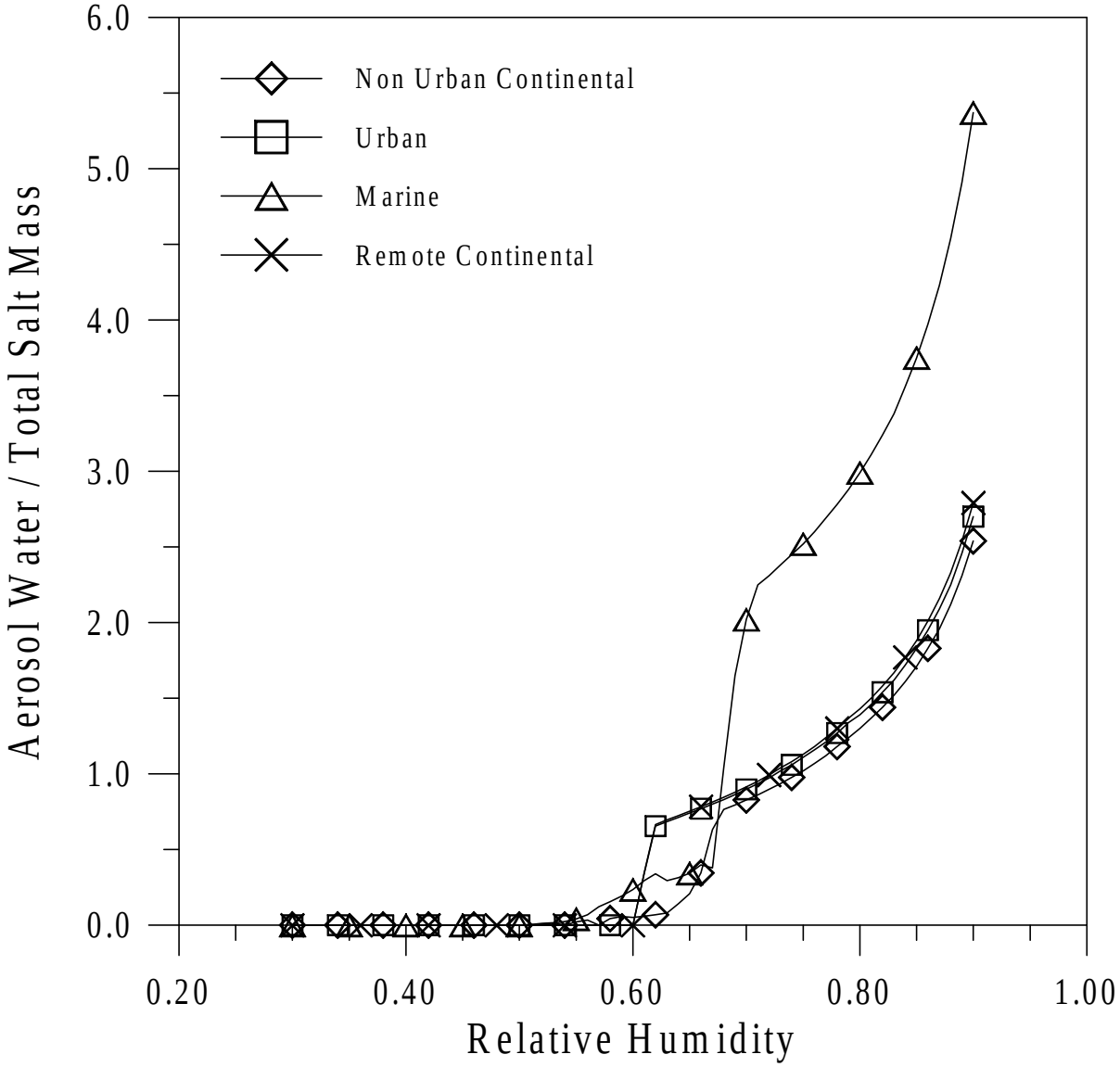
6.0
5.0
4.0
3.0
2.0
1.0
0.0
Aerosol Water / Total Salt Mass
Non Urban Continental
Urban
Marine
Remote Continental
0.20
0.40
0.60
0.80
1.00
Relative Humidity

Figure 11